

---

*Review*

## **A review of the applications of ultra-high performance concrete in flat components and the associated fire-induced spalling risk**

**Xiaodong Cheng<sup>1</sup>, Jun Xia<sup>1,\*</sup>, Theofanis Krevaiakas<sup>1</sup> and Luigi Di Sarno<sup>2</sup>**

<sup>1</sup> Department of Civil Engineering, Xi'an Jiaotong-Liverpool University, Suzhou, 215123, China

<sup>2</sup> Department of Civil and Environmental Engineering, The University of Liverpool, Liverpool, L69 3GQ, United Kingdom

\* **Correspondence:** Email: Jun.Xia@xjtlu.edu.cn.

**Abstract:** In the construction field, ultra-high performance concrete (UHPC) has drawn remarkable attention owing to its outstanding mechanical properties and durability, with increasingly extensive applications in flat components. Moreover, due to its dense microstructure, UHPC is highly susceptible to explosive spalling at elevated temperatures. In this paper, we comprehensively review the application status of UHPC in this domain, encompassing aspects such as bridge deck overlays, composite slabs, steel-concrete composite systems, joint connections, rehabilitation and strengthening, and thin-walled members. We deeply analyzed the spalling mechanisms of UHPC at high temperatures, mostly including thermal stress and vapor pressure mechanisms, and thoroughly investigated influencing factors such as permeability, heating rate, fiber and aggregate types, specimen size, cooling method, external load, and restraint. Additionally, we summarize effective methods to mitigate fire-induced spalling, such as the application of fire insulation, optimization of curing processes, incorporation of fibers or aggregates, and the utilization of thermal spalling-resistant admixtures. Despite the significant potential of UHPC in flat component applications, numerous challenges persist, including further validation of application feasibility, optimization and improvement of interface performance, in-depth elucidation of spalling mechanisms, research and exploration of new fiber materials, full consideration of the scale effect, and exploration and exploitation of innovative improvement solutions for fire resistance. Researchers should concentrate on addressing these issues to promote the broader and more efficient application of UHPC in the construction field.

**Keywords:** UHPC; applications; slab/panel components; fire; spalling; mechanisms; influential factors; mitigation methods

---

## 1. Introduction

Around the globe, concrete has been widely utilized owing to its robustness in strength, favorable durability, and cost-effectiveness and it features lower thermal conductivity and non-combustibility compared to timber and steel materials [1,2]. With the development of cement-based composites and the growing design and performance requirements of building structures, a novel cement-based composite, namely ultra-high performance concrete (UHPC), also known as reactive powder concrete (RPC) or ultra-high-performance fiber-reinforced concrete (UHPFRC) is being widely researched and applied in the construction industry [3,4]. Different from normal strength concrete (NSC) and high strength concrete (HSC), UHPC shows higher tensile strength ( $>7$  MPa), compressive strength ( $>120$  MPa) and excellent ductility [5]. In addition, owing to its great denseness and diminished permeability, UHPC exhibits high durability and reduced maintenance costs [6]. Consequently, UHPC is regarded as an ecologically sound and prospective building material. Given these outstanding mechanical attributes, several UHPC elements are gradually replacing steel or timber structures in some practical construction projects. Besides, UHPC is also used as the supplement to traditional concrete, combining the two to realize significant material and structural advantages. Flat components are a broad concept that refers to components with relatively small thicknesses and large cross-sectional dimensions. They are mainly subjected to bending loads from the structural stress point of view and are very common in engineering applications due to their lightweight design [6]. In recent years, UHPC has been explored for applications in various flat components owing to its unique performance advantages. For example, high crack resistance and extremely low permeability enable UHPC to be an alternative to traditional concrete as an overlay for bridge decks [7,8]. UHPC composite slabs with wood or normal concrete (NC) can maximize the effect while minimizing the usage of UHPC [9–11]. The composite system consisting of UHPC slabs and steel members is one of the key research topics currently being studied [12,13]. In addition, UHPC can serve as an overlay to protect, rehabilitate, and strengthen damaged concrete slabs [14]. With the ever-increasing requirements for building design, prefabricated thin-walled UHPC panels have been developed for applications such as structural and decorative facades/cladding, membrane roofing systems, shading panels, and in-situ formwork [15].

In the service period of a construction structure, fire represents one of the commonly occurring and highly destructive environmental circumstances. Consequently, possessing sufficient fire resistance constitutes a crucial safety prerequisite. The significance of fire resistance for structural components is paramount since it functions as both a primary fire safety requirement within the realm of structural design and a criterion for gauging the likelihood of a structural element failing under fire conditions. Hence, in accordance with prescriptive codes, structural components are typically required to reach a specified fire resistance level, which is ascertained through standardized fire resistance tests following the ISO 834 heating curve. [16]. Studies have experimentally demonstrated that UHPC undergoes a high degree of performance degradation at elevated temperatures and is quite sensitive to explosive spalling because of the highly compact and dense microstructure [17–19]. Two primary inferences have been made as to the cause of spalling behavior: The vapor pressure mechanism and the thermal stress mechanism [20]. UHPC's fire resistance performance is markedly affected by

multiple factors, such as the diverse types and ratios of its ingredients, supplementary materials, different fiber varieties and amounts, specimen dimensions, and curing procedures [21,22]. Nevertheless, the design guidelines and formative principles for preventing spalling in UHPC members require further refinement and extension to better address these aspects [19].

We aim to provide a literature review on the application of UHPC in engineering for flat components and to understand the research directions at the forefront of UHPC. Considering that UHPC demonstrates a high vulnerability to the occurrence of explosive spalling phenomena during exposure to fire, we also summarize and analyze the spalling mechanisms of UHPC at high temperatures, as well as the influencing factors at the material and structural levels. Some effective improvement measures to enhance the fire resistance of UHPC are also compiled, and recommendations for prospective research are provided.

## **2. Applications of UHPC in slab/panel components**

### *2.1. Bridge deck overlays or slabs*

UHPC can be used as an overlay for conventional concrete bridge decks to solve problems such as fatigue cracking, durability deficiencies, and poor load-bearing capacity. An innovative solution to further promote the utilization of UHPC in practical engineering is the implementation of thin UHPC overlays on the new or existing bridge decks [8]. The UHPC overlay cannot only strengthen the structure and organize the corrosive effects of water and chloride ion penetration but also minimize the additional constant loads on the bridge structure [7]. However, the absence of a mechanical connection between UHPC and NC leads to the fact that the bonding between the two types of concrete needs to completely rely on shear friction resistance. Researchers have focused on the evaluation and improvement of bonding properties at different concrete interfaces.

Aaleti et al. [23] performed slant shear tests and flexural tests on UHPC-NC composite deck specimens, which demonstrated that the bond strength across the interface was intimately related to interface roughness, but the concrete strength and the curing conditions showed little effects. Moreover, the research recommended a minimum interface roughness of 3mm (0.12 in.), which has been successfully employed in actual cases. To further increase the adhesion of the interface as well as the serviceability of the UHPC overlay, some scholars have explored and developed some new interfacial techniques, such as an adhesive-based bonding technique [24], a grouped L-shape steel rebar arrangement [25], and a combination of embedded studs and rough surface [26]. Their research also revealed that even thin layers of UHPC can significantly improve the stiffness, crack resistance, abrasion resistance, and durability of the bridge deck.

Orthotropic anisotropic steel decks (OSDs) have been extensively utilized in mid-span and long-span bridge systems owing to the advantages of lightweight, high load-carrying capacity, and construction flexibility [12]. Conventional OSD systems are susceptible to fatigue cracking and lack of durability under repetitive wheel loading due to low local stiffness and stress concentrations resulting from geometric discontinuities at local details [27]. Stresses in the OSD can be reduced by utilizing a concrete overlay integrated with shear connectors on the OSD deck plate to constitute an enhanced stiffness steel-concrete composite section [28]. The excellent properties of UHPC, such as high strength, high crack resistance, and good durability, can compensate for the shortcomings of conventional concrete in the composite structure. A newly proposed steel-UHPC composite bridge

deck (SUCD) system using perfobond strip (PBL) shear connectors possesses a very low deadweight, which facilitates the construction of large-span bridges and lifting during construction, and provides superior ductility, load-bearing capacity, and stiffness to conventional steel-concrete composite slabs [29]. Tan et al. [30] investigated the flexural performance of prefabricated steel-ultra-high-performance concrete composite decks (PSUCD) under transverse hogging moments (as shown in Figure 1). Ten full-scale composite slab specimens were tested, varying shear connectors, steel reinforcement, and wet joint interfaces. Results indicated that notched perfobond strip connectors (NPBLs) with perforating rebars significantly enhanced nominal cracking strength and ultimate capacity compared to studs. The presence of wet joint interfaces reduced nominal cracking strength by up to 26%. Increasing the diameter of surficial reinforcement improved both nominal cracking strength and ultimate capacity. The findings provided valuable insights for the design of UHPC composite decks in bridge construction. To enable further ease of in-situ assembly as well as repair or replacement in case of localized damage, Xiao et al. [31] proposed a prefabricated OSD consisting of standard units and verified its structural performance. Besides, some scholars investigated the mechanical behaviors of ultra-high-performance concrete overlays on composite bridge decks under transverse and longitudinal fatigue loads or negative bending moments by experimental or numerical methods [27,32,33]. A series of studies have greatly promoted the design and development of UHPC in bridge deck slabs, making a rich and powerful theoretical and practical foundation for the applications of SUCD.

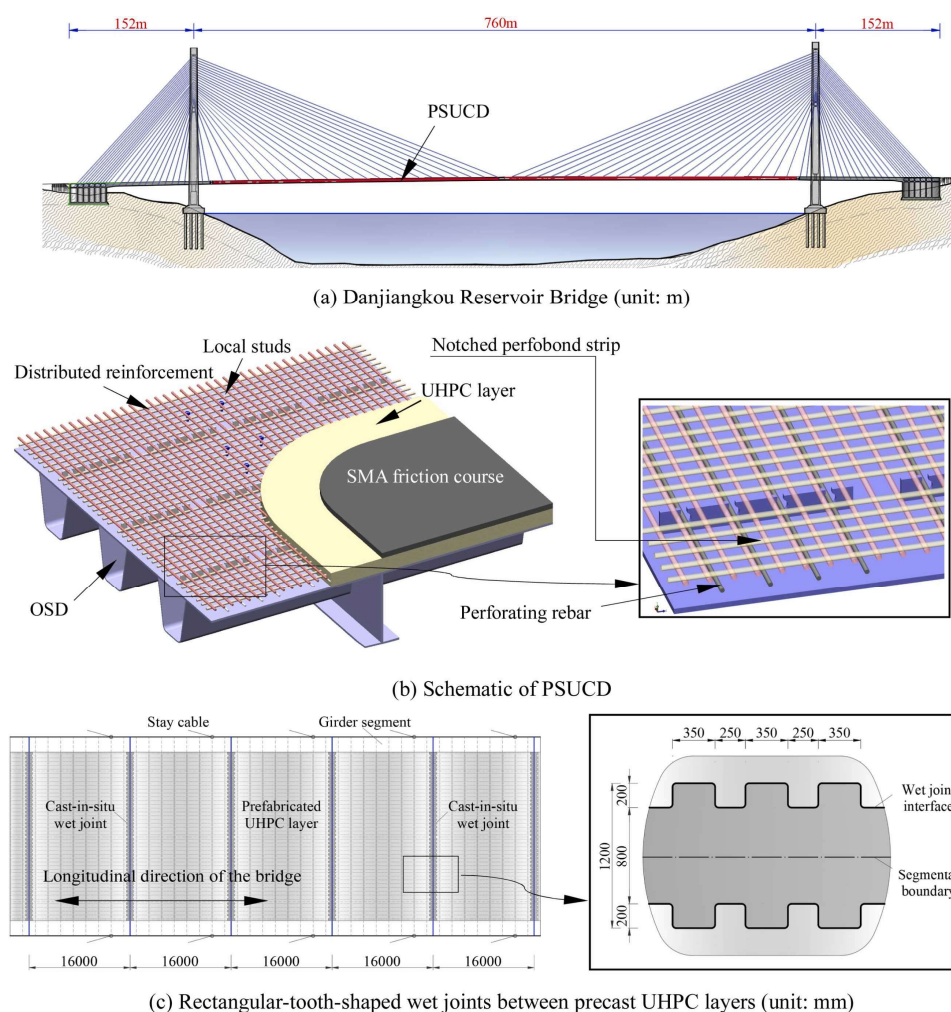


**Figure 1.** Samples of PSUCD (Reproduced from Ref. [30] with permission).

## 2.2. Composite Slab

### 2.2.1. Timber–UHPC composite slab

Timber-concrete composite (TCC) is becoming a popular option for multi-story building floors, benefiting from its advantages in terms of deadweight, structural performance, vibration behavior, acoustic insulation, and environmental friendliness [34]. Several researchers are dedicated to exploring the replacement of conventional concrete with UHPC to utilize the high strength and high Young's modulus of UHPC to improve the stiffness and load-carrying capacity of TCC structures (as shown in Table 1). Lamothe's research team [10,11] validated the practicality and superiority of innovative flooring combining HPC or UHPC with ductile notched connectors with glued laminated timber (GLT) or cross laminated timber (CLT) using experiments, finite element modeling, and predictive modeling methods for plasticity design. Nguyen et al. [35] fabricated two CLT-UHPC floors with a span of 3.6 m to investigate the variation of their deflections under different supported configurations and developed a simplified model to predict the optimal supporting time of the TCC floor. Nevertheless, the limited research is not yet comprehensive enough to provide a theoretical basis for the substitution of UHPC for NSC in TCC slabs, and more in-depth explorations are necessary.

**Table 1.** Summary of experimental parameters from previous research on TCC slabs.

Ref.	Constituent materials (kg/m <sup>3</sup> )	Mechanical property	Geometry of TCC (mm)	Connector
[11]	UHPC: commercial concrete; SF (2%) CLT: Nordic X-lam 175-5s classified E1	UHPC: $f_c = 120$ MPa; $f_t = 8.0$ MPa; $E = 41.2$ GPa CLT: $f_c = 20.7$ MPa; $f_t = 22.1$ MPa; $E = 11.7$ GPa	Span $\times$ width $\times$ thickness = $8000 \times 1000 \times 230$ (55-UHPC + 175-CLT)	Ductile notch connector
[35]	UHPC: cement (555); silica fume (205); glass powder (410); quartz sand (888); HRWR (17); w/b (0.16); SF (2%) CLT: Nordic X-lam 105-3s classified E1	UHPC: $f_c = 98$ MPa; $f_t = 7.8$ MPa; $E = 39.9$ GPa CLT: $f_c = 19.3$ MPa; $f_t = 15.4$ MPa; $E = 11.2$ GPa	Span $\times$ width $\times$ thickness = $3600 \times 1000 \times 145$ (40-UHPC + 105-CLT)	Steel mesh connector

Note: SF-steel fiber (volume); HRWR-high-range water reducer (also known as SP-superplasticizer);  $f_c$ -compressive strength;  $f_t$ -tensile strength;  $E$ -modulus of elasticity.

### 2.2.2. UHPC-NC composite slab

As is widely acknowledged, the expense of UHPC is relatively elevated, rendering it potentially uneconomical to erect an entire edifice using UHPC solely. Thus, it becomes imperative to investigate the judicious utilization of UHPC within NC-UHPC composite slabs (as shown in Table 2). The application of UHPC across the entire depth within a region encompassed by a perimeter at a specific distance from the outer edge of the loading plate surface (as shown in Figure 2) is regarded as the optimal approach for UHPC-NC composite slabs with respect to augmenting the punching shear strength of reinforced concrete flat slabs [36]. Qi's group [37] also verified this conclusion through

punching shear experiments on reinforced concrete flat slabs and proposed a novel energy dissipation ductility index to characterize the post-peak load energy dissipation capacity. Expanding on this conclusion, their group investigated the post-cracking punching behavior of UHPC-NC composite slabs and found that the peak slab strength was reached when the width of the UHPC cover reached a distance of approximately 1-2 times the slab thickness from the periphery of the loading plate [38]. In the study conducted by Kadhim et al. [9], the punching shear performance of hybrid flat slabs, which combine UHPC with NSC, was investigated. The research utilized a finite element model, validated against experimental data, to examine the effects of slab thickness, column size, and UHPC properties on shear capacity. The findings revealed that the area of UHPC significantly bolstered slab strength, and the ratio of UHPC's compressive strength to NC's was a pivotal factor in design considerations. Additionally, the researchers proposed modifications to the American Concrete Institute (ACI) equations to enhance the precision of shear capacity predictions for hybrid slabs.

**Table 2.** Summary of experimental parameters from previous research on UHPC-NC slabs.

Ref.	Constituent materials (kg/m <sup>3</sup> )	Mechanical property	Geometry of slabs (mm)	Connector/interface
[37]	UHPC: cement (732); sand (992); high active admixture (319); SP (22.7); water (176); w/b (0.167); SF (2%) NC: cement (285); sand (757); crushed stone (1003); admixture (195); HRWR (4); water (158)	UHPC: $f_c = 152$ MPa; $f_t = 8.1$ MPa; $E = 49.8$ GPa NC: $f_c = 45$ MPa; $f_t = 3.1$ MPa; $E = 30.5$ GPa	width × width × thickness = 600 × 600 × 60 UHPC width: 80, 200, 320, 440, 600 UHPC depth: 20, 60	HRB 400 steel bar, $\phi 10$ mm
[44]	UHPC: cement (665); quartz sand (1256); silica fume (135); quartz powder (165); SP (21.3); water (138.5); w/b (0.173); SF (2%) UHPC-CB: cement (665); quartz sand (795); silica fume (135); quartz powder (165); CB aggregate (400); SP (19.95); water (151.7); w/b (0.190); SF (2%) NC: cement (495); crushed stone (848); quartz sand (787); SP (1.0); water (194); w/b (0.39)	UHPC: $f_c = 137.1$ MPa; $f_t = 16.6$ MPa; $E = 51.1$ GPa UHPC-CB: $f_c = 142.8$ MPa; $f_t = 17.9$ MPa; $E = 52.6$ GPa NC: $f_c = 45$ MPa; $f_t = 3.1$ MPa; $E = 30.5$ GPa	length × width × thickness = 3000 × 600 × 250 (70-UHPC overlap + 180-NC)	L-shape rebar connectors (ribbed bars with a diameter of 12 mm) Aggregate-exposed treatment (2.6–4 mm) of NC substrate surface
[40]	UHPC: cement (852); silica fume (61); sand (1156); SP (13); water (184); w/b (0.201); SF (2%); PP (0.3%) LWAC: cement (435); active admixture (115); ceramsite (770); SP (11); water (203); w/b (0.369); PP fiber (0.3%)	UHPC: $f_c = 124.1$ MPa; $f_t = 6.8$ MPa; $E = 46.4$ GPa LWAC: $f_c = 16.3$ MPa; $f_t = 1.4$ MPa; $E = 7.5$ GPa	length × width × thickness = 3700 × 900 × 160 (120-UHPC + 40-LWAC)/150 (120-UHPC + 30-LWAC)/160-UHPC	Artificially roughened to enhance the roughness of surfaces

Note: SF-steel fiber (volume); HRWR-high-range water reducer (also known as SP-superplasticizer);  $f_c$ -compressive strength;  $f_t$ -tensile strength;  $E$ -modulus of elasticity; CB-calcined bauxite; PP-polypropylene fiber (volume).

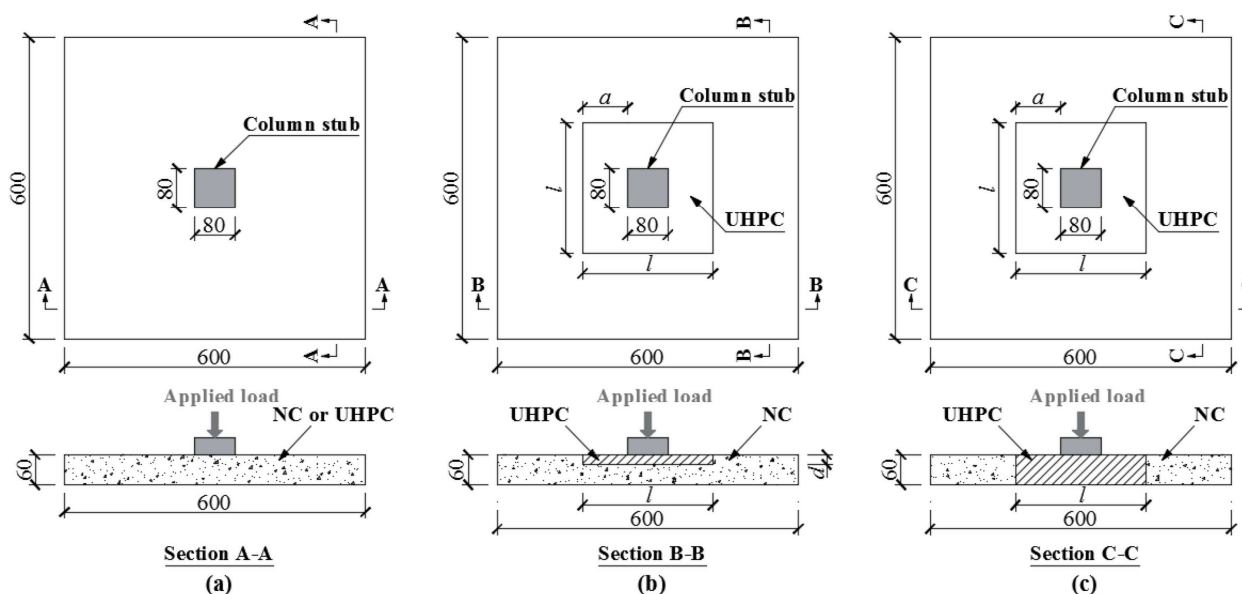


**Figure 2.** Specimen dimensions and layout (unit: mm): (a) NC or UHPC; (b) partial-depth hybrid slab configurations; and (c) full-depth hybrid slab configurations (Reproduced from Ref. [37] with permission).

Functionally graded concrete (FGC) is a cementitious composite whose material composition is spatially variable to meet different performance requirements within the structural component area as well as to reduce cement consumption. It is classified into two major categories: layered or continuous graded concrete [39]. Du et al. [40] designed a two-layered FGC slab consisting of a UHPC layer serving as the structural layer to carry the loads and a lightweight aggregate concrete (LWAC) layer for thermal insulation, and applied it to the smoke duct slabs of the Haitai Yangtze River Tunnel in Suzhou, China (as shown in Figure 3). This composite structure can take full advantage of the outstanding mechanical properties of UHPC and the thermal properties of LWAC and enables the removal of additional fire protection technologies such as insulation boards or coatings. Their research team also evaluated its interfacial properties at ambient and elevated temperatures through debonding tests and examined the effect of casting bolts [41]. Yan et al. [42] developed an innovative UHPC-reinforced concrete (RC) composite deck slab. This design featured prefabricated UHPC T-beams, either single or double, placed at the bottom of cast-in-place concrete of conventional strength, thereby boosting the slab's span capacity. Full-scale experimental tests revealed that the UHPC-RC composite outperformed standard RC deck slabs in crack resistance, flexural stiffness, and load-bearing capacity while also effectively limiting crack expansion.

These optimized methods of UHPC in combination with other concrete have been successfully implemented in practical engineering and on-site validation, which minimize the usage of UHPC while taking full advantage of the material benefits of UHPC to minimize costs. Pursuing cost-effective solutions to promote the widespread application of UHPC is one of the top priorities.



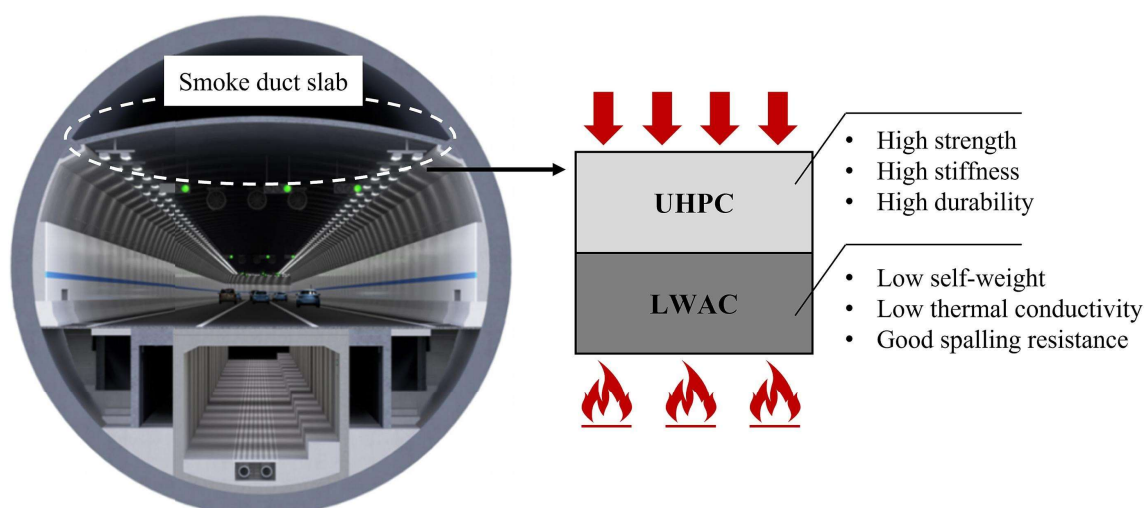


**Figure 3.** FGC smoke duct slab in the Haitai Yangtze River Tunnel (Reproduced from Ref. [40] with permission).

Given that the UHPC overlay exhibits a significant degree of autogenous shrinkage and a relatively low creep coefficient in contrast to ordinary concrete, it has the potential to render the UHPC-NC composite slabs susceptible to interface debonding and warping distortion [43]. Guo et al. [44] applied groups of L-shaped rebar connectors to restrain the shrinkage and creep of UHPC layers, and the results proved that the warping and delamination of UHPC-NC composite slabs were effectively mitigated. Liu et al. [45] explored the potential of calcined bauxite (CB) as an internal curing agent to reduce autogenous shrinkage in UHPC. The research demonstrated that UHPC with CB aggregate exhibited delayed cracking and reduced crack widths, enhancing its mechanical properties and durability. These innovations extend the promise of UHPC in traditional concrete surface overlays and structural rehabilitation, overcoming the disadvantages of autogenous shrinkage inherent in UHPC materials. It is worth noting that the lack of a convenient and intuitive hybrid element design model in design codes hinders designers from employing UHPC overlays in practical construction applications. Thus, Pharand et al. [14] developed a simplified cross-sectional analysis prediction model for NC-UHPC hybrid members based on existing codes and proposed a simple and expedient empirical equation to evaluate the maximum flexural capacity of hybrid elements.

### 2.3. UHPC-steel composite system

Steel-concrete composite structures are widely used in building structures, including composite beams, composite slabs, and composite columns, due to the advantages of making full use of the respective properties of steel and concrete materials through different structural forms, which have the advantages of low deadweight, high mechanical properties and cost-effectiveness [46,47]. In recent years, some researchers in the field of composite structures with UHPC slabs and steel have focused on two major issues: (i) the performance of shear connectors for composite beams composed of UHPC slabs and steel; and (ii) the structural behavior of composite slabs composed of UHPC and steel in different forms.



Zhang et al. [48] explored the shear characteristics of clustered single-embedded-nut high-strength bolts (SENHSBs) in steel-UHPC composite slabs (as shown in Figure 4). The research project, which incorporated both practical experimental push-out investigations and detailed numerical simulations, uncovered that the SENHSB fracture predominantly dictated the failure modality. It was ascertained that the longitudinal gap exerted a pronounced effect on the peak shear and sliding potential, whereas the transverse interval had an impact on the shear firmness and the maximal slippage. Xu et al. [49] explored the flexural performance of steel-UHPC composite beams with ultrathin UHPC slabs and ultrashort stud connections. Their previous research concluded that short-stud UHPC connections exhibit greater slip rigidity compared to those with conventional concrete [50]. The experimental analysis revealed that variations in stud spacing, slab thickness, and stud aspect ratio significantly influenced the beams' moment capacities, deflection increments, and failure modes. It suggested that ultrathin UHPC slabs can provide comparable elastic flexural stiffness to thicker conventional slabs, with enhanced ductility, and that current design codes can accurately predict the bearing capacity of such composite systems. In addition, their subject group also investigated the shear behavior of other types of bolt connections, such as large-diameter bolts [51], large-diameter high-strength friction bolts [52], and wedge block-crossed inclined studs [53], to provide a basis and guidance for the application of thin UHPC slab-steel beam composite structure connections.

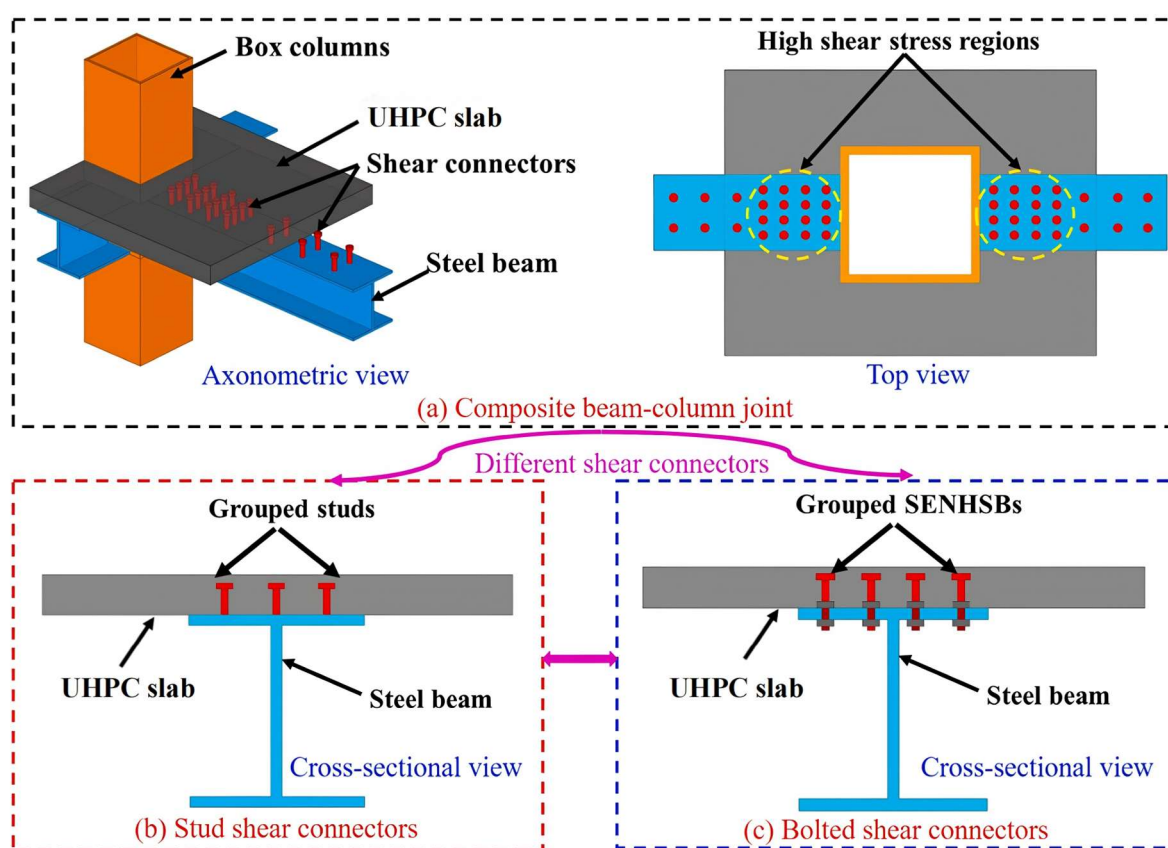


**Figure 4.** Schematic of steel-concrete composite beams (Reproduced from Ref. [48] with permission).

A steel-concrete-steel (SCS) composite structure is a popular sandwich structure made of concrete cast between two steel plates with shear connectors on the inside (as shown in Figure 5). The steel plates on the two sides act as formwork with a membrane effect, resisting deformation and cracking of the concrete, while the concrete on the inside prevents buckling of the steel plates and strengthens stability. The research team of Wang et al. [54] performed a series of mechanical tests and studies on SCS composite slabs with different loadings, such as concentrated loading, ultimate loading [55], and low-velocity impact [56]. They carried out detailed analyses of the structural response, damage modes and failure mechanisms, and then developed finite element models for parametric analysis. Eventually, they proposed prediction models and design methodologies based on different working conditions [57]. A series of studies have verified the ability of SCS composite slabs in various aspects, providing experimental and theoretical support for the promotion and application of SCS composite slabs. Due to its excellent impact and blast resistance, as well as its remarkable assembly and construction efficiency, SCS sandwich composite structures are extended in applications such as new-generation nuclear power plants [58], shield tunnels [59], shear walls [60,61], and protective structures [62].

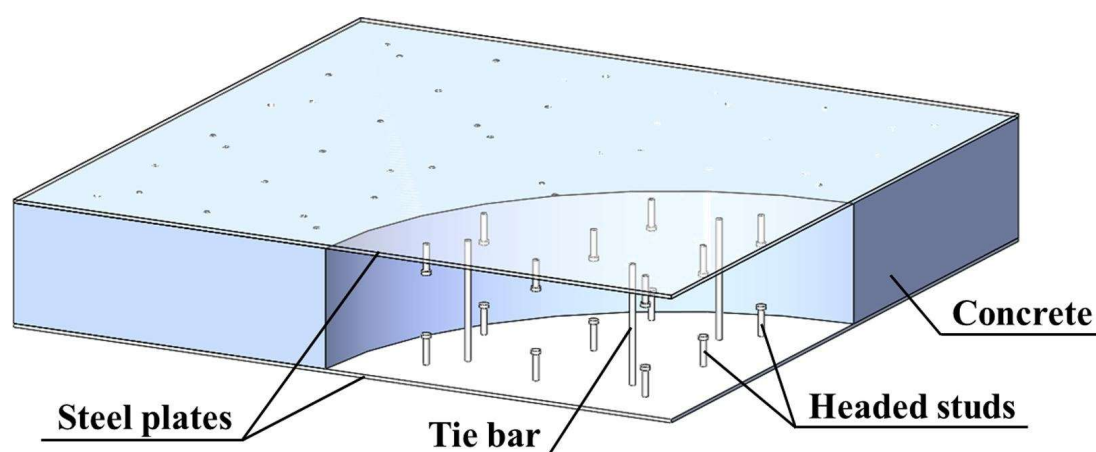


**Figure 5.** Schematic of steel-concrete-steel composite slabs (Reproduced from Ref. [55] with permission).

#### 2.4. Joint or connection

UHPC possesses the characteristics of self-compaction and ease of construction. Moreover, it can attain high strength within a brief period, thus fulfilling the requirements of rapid construction projects. Furthermore, owing to its exceptional mechanical properties, UHPC is increasingly being utilized to solve engineering problems at the connections or joints of bridge members.

Qiu et al. [63] presented an experimental study on full-scale UHPC slabs, focusing on failure modes, load-displacement response, and cracking behavior. They varied joint shape, steel reinforcement diameter, joint interface roughness, and constraint conditions, such as fixing both ends of the specimen with bolts (Figure 6a) or freely supporting it on the ground (Figure 6b). The findings suggested that T-shaped joints enhanced flexural behavior compared to rectangular joints, and increasing steel diameter improved performance. Wang et al. [64] proposed a narrower, six cm-wide UHPC joint, which simplified reinforcement arrangements and reduced construction complexity compared to traditional epoxy joints. Experimental and numerical analyses demonstrated that the compact UHPC

joints provided comparable shear resistance to epoxy joints, with enhanced ductility and load distribution between precast panels. Hu et al. [65] introduced an innovative joint utilizing UHPC and carbon fiber-reinforced polymer (CFRP). Their research, conducted through static monotonic experiments on full-scale precast concrete deck panels (PCDPs) and complemented by finite element analysis, revealed that the proposed joints exhibited enhanced deformation capabilities and a more favorable failure mode compared to conventional joints. Subsequently, their research team also conducted fatigue bending tests on the proposed high-performance connection and developed prediction models for estimating cracking moments, deflections, fatigue deflections, and fatigue damage quantities [66,67]. The findings provided valuable insights for the design of durable PBDPs in bridge construction and highlighted the positive influence of CFRP tendons and UHPC grout on the structural performance under bending moments. Qi et al. [68] examine the flexural behavior of a newly developed dovetail UHPC joint within composite bridges subjected to negative bending moments. A fresh approach to interface treatment, utilizing steel wire mesh (SWM), was implemented, augmenting the mechanical interlocking mechanism between precast and cast-in-place UHPC. The research findings indicated that the SWM technique substantially enhanced the joint's nominal cracking strength by 2.4 MPa and sustained the post-cracking rigidity at around 80% of the initial stiffness value.

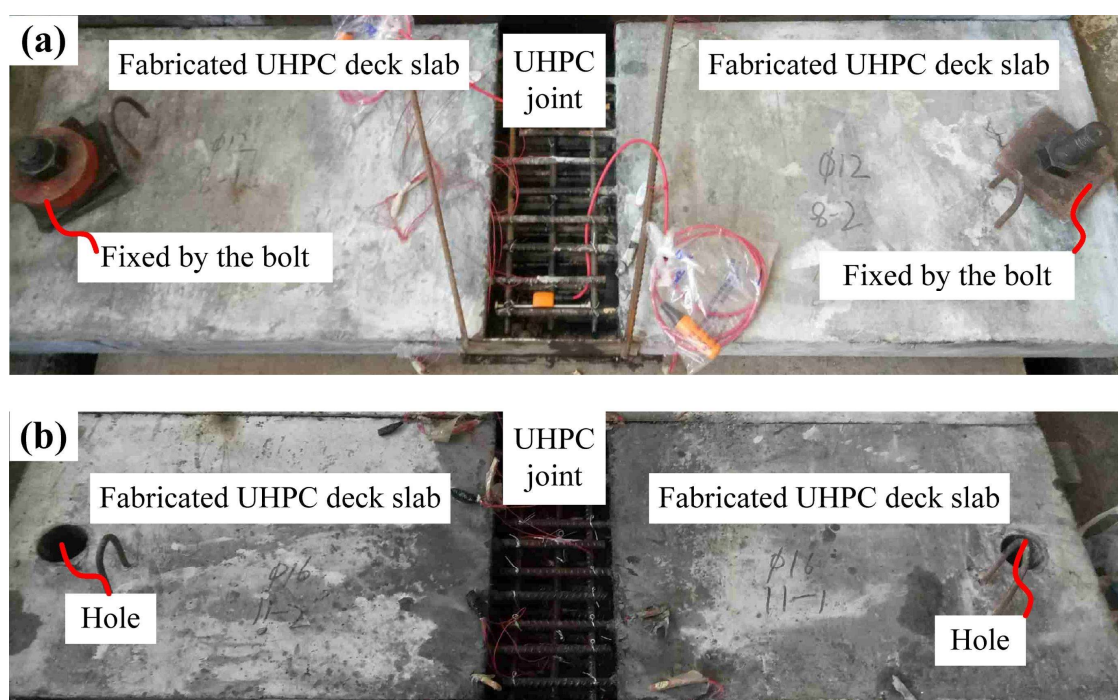


**Figure 6.** Diagram of precast UHPC slab and cast-in-place joint with different constraints: (a) fixed; and (b) free (Reproduced from Ref. [63] with permission).

These studies on the application of UHPC in the joint connection of precast concrete slabs provide reference and guidance for the design and construction of practical constructions, but cannot support all the diverse and complex engineering problems.

## 2.5. Rehabilitation and strengthening

UHPC has been demonstrated to be a viable alternative for the reinforcement of degraded reinforced concrete structures. This material is capable of not only augmenting the flexural strength and ductility but also enhancing the permeability resistance and durability of the reinforced framework.

Pharand et al. [69] summarized four basic configurations for slabs combining UHPC and NSC according to functions (as shown in Figure 7) based on other studies: Protection, rehabilitation, and strengthening. Figure 7a shows that the P configuration aims to shield the NSC against moisture and chloride penetration. This is achieved by applying a UHPC layer with a thickness varying between 25 and 40 millimeters positioned atop the NSC's upper tensile reinforcement stratum. The R configuration is designed to address scenarios where the reinforcement bars are diminished due to corrosion, necessitating slab restoration. A UHPC layer no less than 40 millimeters thick is designed to encapsulate the rebars, preserving the initial thickness of the slab, as depicted in Figure 7b. This layer may also incorporate fresh reinforcement bars to make up for the corroded area. For the S setup, which serves to strengthen the element, a UHPC layer exceeding 40 millimeters in thickness is installed over the NSC's upper tensile reinforcement layer, resulting in an augmented cross-sectional thickness ( $\Delta h$ ), as shown in Figure 7c. This layer is further bolstered by new reinforcement bars. Last, the RS setup combines both rehabilitation and strengthening functions. It employs a UHPC layer similar to the "R" configuration, preserving the dimensions of the original cross-section. However, the additional reinforcement bars introduced not only replace the corroded sections but also enhance the overall structural strength, as illustrated in Figure 7d.

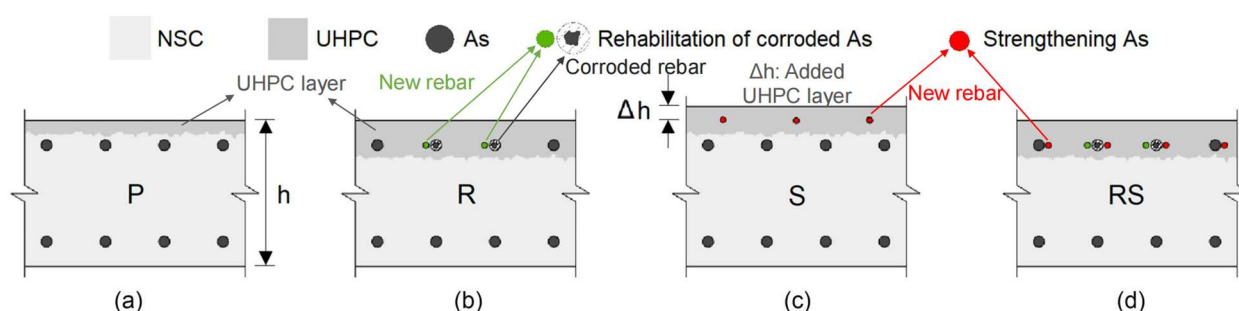


**Figure 7.** Basic hybrid NSC-UHPC configurations depending on functions: (a) protection; (b) rehabilitation; (c) strengthening; and (d) rehabilitation and strengthening (Reproduced from Ref. [69] with permission).

Zhu et al. [26] explored the efficacy of UHPC overlays in enhancing the flexural strength of large-scale, pre-damaged reinforced concrete bridge slabs. Employing two distinct interface treatments—embedded studs with roughened surface (S-R) and rough surface alone—the research demonstrated that UHPC overlays significantly increased both the cracking and ultimate loads. The S-R technique, in particular, provided a notable improvement in load capacity and stiffness, underscoring the potential of UHPC overlays in bridge rehabilitation to restore and augment structural performance. Besides, they [70] provided a detailed finite element analysis of damaged RC slabs that were then strengthened with a UHPC layer. The study meticulously modeled pre-existing cracks in the RC substrate and incorporated a UHPC-RC interfacial model to simulate the bonding strength between the two different materials. Validated against experimental results, the FE model demonstrated the

significant impact of existing cracks on the ultimate flexural capacity of the composite slab. Furthermore, the research included a parametric study to optimize strengthening parameters, enhancing the understanding of UHPC-RC composite behavior under flexural loading. Teng et al. [71] investigated the flexural performance of reinforced concrete slabs repaired with UHPC-bonded overlays of different thicknesses (25, 38, and 50 mm) and steel fiber volumes (2% and 3.25%). The results indicated an improvement in the cracking load by at least three times and in the flexural capacity by more than 35% compared to latex-modified concrete (LMC).

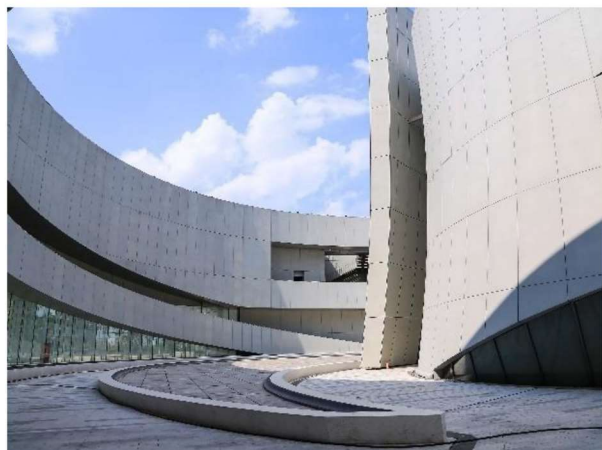
While the studies provide valuable insights into UHPC's capabilities, there is a need for more comprehensive research on long-term durability, cost-effectiveness, and practical implementation strategies for UHPC overlays in various environmental conditions and structural scenarios. Further exploration into the optimization of UHPC compositions and configurations could lead to more efficient and economical rehabilitation solutions. Additionally, the development of standardized guidelines for UHPC application in different structural contexts would be beneficial for the industry.

## 2.6. *Thin-walled member*

In recent years, with the continuous advancement of building modernization, there has been an increasing demand for lightweight exterior panels to meet environmental conditions and adapt to the various shapes and aesthetic requirements of irregularly shaped buildings (as shown in Figure 8). The prefabricated UHPC panels have become increasingly popular with architects and engineers as building envelope materials due to their superior structural performance and flexibility [15].

UHPC offers many advantages as an exterior panel, e.g., (1) easy formation into ultra-thin shapes and customizable surface textures; (2) lighter, thinner and stronger structural performance compared to traditional stone and concrete; (3) resistance to chlorine erosion and high durability; and (4) low sensitivity to environments with complex climates [72]. Based on these benefits and the development requirements of the construction industry, thin-walled UHPC panels have been implemented in applications such as structural and decorative facades/cladding, membrane roofing systems, shading panels and stay-in-place formwork. There are examples of projects worldwide where UHPC panels have been used, e.g. the facade at Terminal 1 of Rabat Airport in Morocco [73], the cladding for the Fondation Louis Vuitton Pour La Creation Iceberg in Paris [74], the cladding for the Qatar National Museum [75], the roof system for the Olympic museum at Lausanne, Switzerland [76], and the precast thin curve shells at a French wastewater treatment facility [77]. Nevertheless, the promotion of UHPC thin panels has been somewhat hindered by the restricted design specifications and guidelines, the lack of details regarding raw materials and manufacturing techniques, as well as the high production expenses [78].





Ningbo Fenghua Future City Science Center,  
China  
(<http://tongchuanguhpc.com>)



Foundation Louis Vuitton Pour La Creation  
Iceberg, France  
(<https://www.fondationlouisvuitton.fr>)



Westlake University, China  
(<https://www.goood.cn>)



Museum of European and Mediterranean  
Civilization, France  
(<http://www.mucem.org>)



Roof of the Guibournein Stadium, France  
(<http://www.meady.com.cn>)



Apple Scottsdale Fashion Square Ceiling  
(<https://mmbiz.qpic.cn>)

**Figure 8.** Applications of thin UHPC members.

Harsono et al. [79] examined the integration of design and fabrication in the construction of building facades using prefabricated (UHPC) panels. They highlighted the challenges of adopting UHPC due to factors such as cost, complexity of fabrication, and industry unfamiliarity. Their study also advocated for the use of digital technologies to facilitate communication and collaboration across disciplines, thereby optimizing the design and installation process of UHPC panels. Kim et al. [72] examined the impact resistance of UHPC facades, comparing white-colored UHPC with non-colored variants and granite. It was found that UHPC, particularly when incorporating steel fibers, exhibited superior impact performance, resisting high-velocity impacts better than granite. This resilience is attributed to UHPC's ductility and the bridging effect of steel fibers, which prevent brittle failure and reduce the secondary damage from debris. The study suggests UHPC as a viable material for facades, offering enhanced protection for structures against environmental and impact loads. In addition, Leone et al. [80] presented a comprehensive design methodology and digital workflow for optimizing the production and performance of UHPC shading panels. By incorporating site-specific data related to climate, urban context, and material properties, the developed workflow enabled the creation of customized shading solutions that enhanced indoor thermal comfort and daylight performance while reducing manufacturing costs. A novel composite roofing system, which has been devised to endure hurricanes, has been put forward for application in industrial, commercial, and residential buildings [81]. It integrates UHPC and high-strength steel (HSS) to create a lightweight, low-profile, and thin-walled structure without the need for transverse or shear reinforcement. The research indicates that the proposed roofing system offers an optimal balance of strength and economy, with significant potential for enhancing the resilience of buildings against severe wind events.

The development of thin UHPC panels is in a nascent stage, and research in this area is limited. Hence, there is an urgent demand for scholars and engineers to work together to find innovative solutions to promote the application.

### 3. Mechanisms and influential factors of fire-induced spalling

Studies have indicated that compared with conventional concrete, UHPC is more susceptible to spalling under fire and high-temperature circumstances. Consequently, the load-bearing capacity of the structure is significantly reduced, posing a threat to its safety. There are two commonly recognized mechanisms for explaining the spalling of HSC and NSC at elevated temperatures [20,22]. The first is the thermal dilation and stress mechanism. Rapid temperature fluctuations and high thermal gradients generate high-stress gradients, potentially causing the concrete material to reach its failure limit, as illustrated in Figure 9a. However, this mechanism is not applicable to low heat rate ambient conditions, and the thermal stress is also related to Young's modulus and transient thermal strain of the concrete. Given that UHPC has high tensile strength ( $>7$  MPa) and compressive strength ( $>120$  MPa), the validity of this explanation demands further experimental and analytical verification. The high vapor pressure mechanism might be another possible cause of concrete spalling, as shown in Figure 9b. The accumulation of 'moisture blockage' and water vapor pressure within the concrete pores is regarded as the main factor contributing to explosive spalling [82–84]. Figure 9c presents a spalling description combining thermal stresses and pore pressure. Liu et al. [85] analyzed conflicting and consistent test results from previous fire-induced concrete spalling research efforts. They proposed a unified spalling theory that classifies the spalling mechanisms into three types: thermo-hygral, thermo-mechanical and thermo-chemical spalling. Thermo-hydral spalling (typically occurs within 220 and 320 °C) and



thermo-mechanical spalling (typically occurs within 430 and 660 °C) are related to pore pressure buildup and restraint-induced thermal stress, respectively. These two types have similarities with the two mechanisms mentioned earlier. The last one is thermo-chemical spalling, which was categorized into two cases: one is under extreme high temperatures (estimated over 700 °C), where the aggregate-cement paste bond is severely damaged and results in sloughing-off spalling [85,86]. The other is post-cooling spalling after exposure to very high temperatures. High-temperature heating decomposes calcium carbonate in calcareous aggregate into calcium oxide. After cooling, absorbed moisture from the air reacts with the surface calcium oxide, causing the rehydration of calcium oxide and expansion of aggregates in concrete [87,88]. However, it is worth noting that this unified spalling theory has not yet been comprehensively verified by experimentation [22]. The mechanisms relating to extreme high temperatures and post-cooling spalling deserve further investigation.

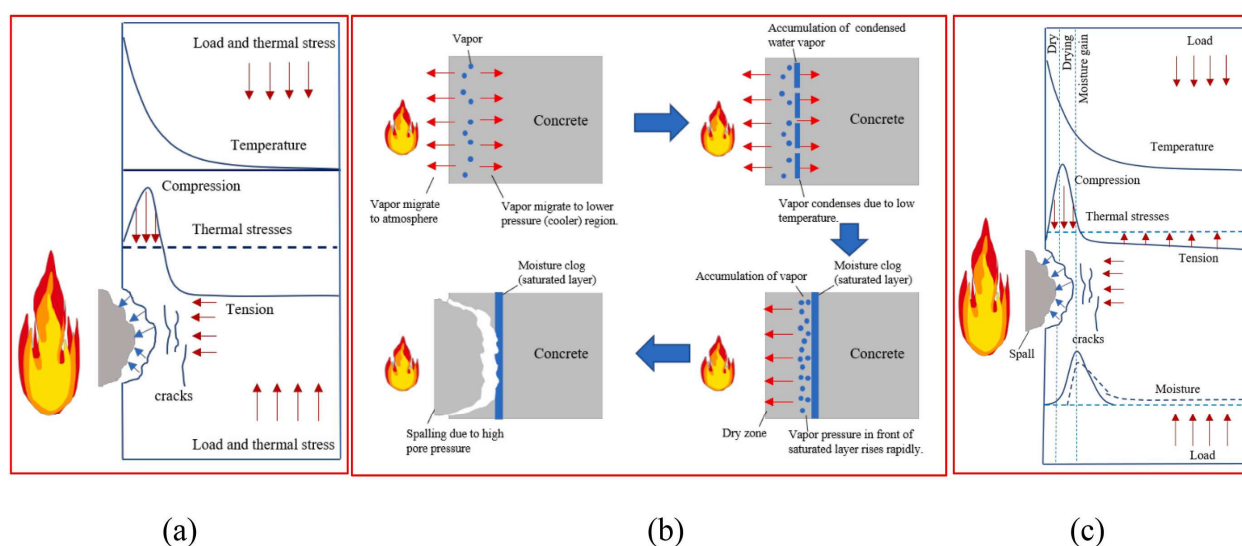


**Figure 9.** Description of the spalling due to (a) thermal stresses, (b) pore pressure, and (c) combined thermal stresses and pore pressure (Reproduced from Ref. [22] with permission).

Researchers have explored the effect of testing parameters on the fire performance and spalling behavior of UHPC [21,22]. These parameters can be classified into multiple categories, namely material, structural, mechanical, and temperature aspects. According to the documented literature, in this section, we will present a short overview of the factors influencing the behavior of fire-induced spalling, with Table S1 and S2 in Supporting information summarizing the material parameters and test parameters from the previous literature, respectively.

### 3.1. Permeability

The migration of moisture within concrete is inherently linked to its permeability characteristics. Concrete with low permeability tends to evacuate moisture at a slower rate, which can lead to the accumulation of pore pressure. This phenomenon is particularly critical as it heightens the risk of thermo-hygral spalling, a process where rapid temperature changes cause the trapped moisture to expand, leading to potential surface flaking or spalling of the concrete [85]. UHPC is more prone to spalling than conventional concrete as it has a lower permeability and a denser microstructure [89]. With numerous studies on the role of adding polymer fibers to UHPC, it is now believed that three key

mechanisms explain the increased permeability of UHPC driven by exposure of polymer fibers to high temperatures [19]: (i) polymer fiber melting: the thermal dissolution of polymer fibers within the UHPC matrix is theorized to culminate in the establishment of a network of porous pathways [90]. This phenomenon contributes to a decrement in pore pressure, thereby substantially enhancing the material's resilience against spalling. (ii) Pressure-induced tangential space (PITS): the core of this mechanism lies in the polarity incongruence between the matrix and fibers or the fibers and moisture. Upon reaching temperatures over 100 °C, the vapor pressure generated is capable of swiftly disintegrating the interfacial zones that are formed as a result of this polarity misalignment [91]. (iii) Differential thermal expansion of fiber and matrix: the thermal equilibrium between the fibers and the matrix may induce microcracking at their juncture, which is postulated as an additional avenue for the mitigation of vapor pressure within the UHPC matrix.

### 3.2. Heating rate

The heating rate can influence the spalling behavior and mode of high-performance concrete, the reason being that an increase in heating rate alters the temperature gradient and vapor pressure on the stress distribution and damage pattern [92]. The heating rate affects the extent of pressure build-up inside the sample: faster heating indicates faster vaporization and higher peak pore pressures, while thermal-induced fracture tends to augment gas permeation and pressure release [93]. According to the findings of Liang et al. [94], a higher heating rate might lead to more intense explosive spalling as the rate of heating increases with earlier onset and end of explosive spalling. Their group experimentally demonstrated that due to the dense nature of UHPC, with a slow release of vapors, excessive heating rates could cause explosive spalling between 320 and 380 °C [95]. Nevertheless, after turning down the heating rate to 5 °C/min, there was some chance of spalling. Furthermore, high heating rates are usually conducted for spalling studies to measure mass loss as well as structural behavior after the target temperature has been reached, and low heating rates allow for easier strength assessment [96] because low heat rates mitigate the generation of undesirable temperature gradients inside the specimen to reduce spalling in a specific temperature range [82,97]. The spalling witnessed in tests with slow heating rates cannot be accounted for by the mechanisms applicable to fire conditions. In slow heating scenarios, the spalling of concrete might be due to extremely high vapor and liquid water pressures resulting from the saturation of internal pores with water [22].

The ISO 834 heating curve [16] is used to simulate fire scenarios for building elements, where the temperature-time curve is defined as  $T = 20 + 345\log(8t + 1)$ . This international standard heating profile gives an average rate of 67.8 °C /min for the first ten minutes, which is close to the severity of real fire conditions. It can be seen that the rate of heating has a critical impact on UHPC spalling. Thus, it is essential to develop suitable strategies to manage the rate at which the concrete temperature rises to ensure that it meets the required performance. Further research is needed to fully understand how the heating rate affects the UHPC spalling mechanism, as the quantitative evaluation of the heating rate is yet insufficient.

### 3.3. Incorporation of fibers or aggregates

#### 3.3.1. Different fibers

The effect of material parameters such as aggregate type, fiber type (as shown in Table 3), and chemical composition have been explored in previous investigations to improve the fire performance and spalling of UHPC.

**Table 3.** Summary of the role of different fibers in UHPC spalling resistance.

Type of fiber	Melting point (°C)	Density (kg/m <sup>3</sup> )	Anti-spalling efficiency
Steel fiber	1450–1500	7850	Effective [100] but controversial [101]
PP fiber	163–175	890–910	Effective [83], better mixed with steel fiber [96]
PVA fiber	225–230	1260–1300	Effective [112]
Jute fiber	220	1100	Effective and dosage-dependent [107]
PE fiber	124–138	950–960	Not as good as PVA and PP fibers [112]
PET fiber	257–265	1380–1410	Not as good as PP fiber [113]
PA/Ny fiber	263	1150	Effective [110]
PAN fiber	220	1140–1180	Not as good as PP fiber [108]
LLDPE	120–125	925	Effective [110]
UHMWPE	145–160	970	Ineffective [110]

Note: PP-polypropylene; PVA-polyvinyl alcohol; PE-polyethylene; PET-polyester; Ny-nylon; PA-polyamide; PAN-acrylic; LLDPE-linear low-density polyethylene; UHMWPE-ultra-high molecular weight polyethylene; CF-carbon fiber.

The incorporation of steel fibers can effectively improve the compressive and flexural strength of UHPC, as well as inhibit the development of brittle failure, and the most efficacious and economical amount of steel fibers added at high temperatures is 2.0%–2.5% [98]. It has been shown that steel fibers have a bridging effect below 600 °C, which improves the mechanical properties of UHPC. The steel fiber mitigates spalling caused by thermal stress and incompatibility between the aggregate and the cement paste [94]. Abid et al. and Zheng et al. [99,100] also demonstrated the effectiveness of steel fibers in preventing explosive spalling. They ascribed this efficacy to the fact that the steel fibers possess a higher thermal conductivity than the cement matrix. This enables more efficient heat transfer within the steel fibers, thereby reducing the overall disparity in thermal stress among various parts of the concrete specimens by diminishing the thermal gradient. However, in several experiments, the effectiveness of the single-doped steel fibers in enhancing the explosive spalling resistance of UHPC is not satisfactory enough [101]. The probability of spalling grew as the volume content of steel fibers increased. This might be because the permeability wasn't augmented, and the pore pressure did not decrease at high temperatures in the presence of steel fibers [89,102]. The mechanism of using steel fibers to avoid or improve the risk of spalling remains to be further investigated.

Li et al. [102] studied the performance of intrinsic permeability of UHPC containing aggregates of different sizes and various contents of PP and steel fibers at temperatures up to 300 °C. Results

revealed that the use of PP fibers together with larger aggregates in UHPC exhibited a synergistic effect and contributed to a significant increase in permeability at high temperatures. This is due to the melting and thermal expansion of the PP fibers and the mismatch between the aggregate/fibers and the cement matrix, which forms an interconnected network of microcracks. Zhang et al. [83] experimentally demonstrated that the empty channels of PP fibers do not have a dominant contribution to the permeability of concrete and reaffirmed the significance of the formation of interconnected crack networks at temperatures below the fiber melting point. However, PP fibers could decompose into pentane and propylene at temperatures in the range of 360–400 °C, which increased the pore pressure and impeded the release of vapor, hence increasing the risk of explosive spalling of UHPC [22]. Moreover, Sciarretta et al. [96] showed that the use of PP fibers alone does not always alleviate the occurrence of UHPC spalling and that hybrid PP and steel fibers have better action. The content and length-to-diameter ratio of PP fibers are essential parameters affecting the explosive spalling resistance of UHPC reinforced with hybrid steel and PP fibers, and the extent of explosive spalling decreases with increasing PP fiber content ( $\leq 0.3\%$ ) and length-to-diameter ratio ( $\leq 633$ ) [101]. It has also been confirmed in another research that when using 3 kg/m<sup>3</sup> of PP fibers, the L/D ratio of 300 is the critical value for UHPC spalling protection and that longer and finer PP fibers seem to be more effective [103]. Huang et al. [104] revealed experimentally that the compressive loading failure modes of C120 UHPC with hybrid steel and PP fibers were varied under different temperatures and that the compressive strength increased with temperature from 20 to 200 °C and decreased with temperature in the range from 200 to 800 °C. The microscopic investigation indicates that this is mainly due to the higher temperatures promoting cement hydration and pozzolanic reaction [105].

It has been observed that the incorporation of SF alone does not prevent explosive spalling, while the mixing of PP, polyvinyl alcohol fiber (PVA), and jute fibers (JF) with SF gives excellent results [106]. In addition, substituting PVA with an equal volume fraction of SF is the optimal substitution ratio, which minimizes the effect on the mechanical properties of UHPC and maximizes the prevention of explosive spalling. Zhang et al. [107] researched the addition of different dosages of natural fibers (jute fibers) into UHPC to observe the performance and behavior of the specimens exposed to high temperatures. Different from synthetic fibers (PP and steel fibers), as the temperature increases, the jute fibers gradually shrink and then form interfacial gaps between the fibers and the cement matrix, increasing the hot permeability of UHPC. Some researchers have also discussed the role of PVA, polyethylene fiber (PE), and nylon fiber (Ny) concerning improving the fire resistance and mechanical properties of UHPC [17,108], as well as the influence of the chemical composition of the concrete on spalling behavior [109].

Zhang et al.'s group [110] investigated the effect of a series of different types of polymer fibers, such as PP, polyester (PET), polyamide (PA), linear low-density polyethylene (LLDPE), and ultra-high molecular weight polyethylene (UHMWPE) fibers on the pore pressure and spalling behavior of UHPC specimens exposed to high temperatures. It was shown that the growth of pore pressure is the main cause of UHPC spalling and that the polymer fibers strengthen the spalling resistance by influencing the development of the pore pressure rather than the temperature gradient and moisture content. Specifically, when PET, LLDPE, PP, and PA fibers were subjected to elevated temperatures, their expansion generated micro-cracks. These cracks enabled the movement of moisture within the UHPC sample. PET fibers had a tendency to cause 'moisture blockage' inside the specimen, while LLDPE fibers transported moisture to deeper regions. Collectively, these processes culminated in the accumulation of pore pressure at greater depths, subsequently resulting in the detachment of the entire UHPC layer. It is proposed that fibers possessing a relatively high coefficient of thermal expansion

within the 100–200 °C range, such as PP and PA fibers, are advantageous for mitigating pore pressure and preventing spalling phenomena. Zhang et al. [111] developed two types of synergistic flame-retardant polymer (SFRP) fibers, organic polymer fiber (OP) and modified polymer fiber (MP), and examined several physical and chemical properties of them. A series of high-temperature tests demonstrate that the addition of SFRP fibers has a significant improvement in the residual modulus of elasticity, residual compressive strength, explosive spalling, damage modes, and thermal performance and efficiency in terms of thermally induced damage of UHPC. This can be attributed to the enhancement of pore connectivity, filling of pores/cracks by flame retardant polymers caused by thermal stresses, and delayed degradation of micromechanical performance.

### 3.3.2. Different aggregates

UHPC is primarily composed of fine-grained powders with high activity to achieve extremely high packing densities for outstanding performance [22]. As a result, the overall cost of UHPC remains high, and researchers have experimented with and validated methods of incorporating aggregates to reduce costs while maintaining excellent properties. Most UHPCs use fine aggregates with a typical size of less than 0.6 mm, which improves the homogeneity of the powder blend and minimizes interfacial transition zones [114]. Similar to fibers, the role of different types of aggregates on the spalling resistance of UHPC is also under investigation. Yang et al. [115] investigated the explosive spalling behavior of UHPC with and without coarse aggregate (CA) when exposed to high temperatures. It was found that the inclusion of coarse aggregate slightly mitigated the spalling, which is attributed to the fact that coarse aggregates can reduce the thermal stresses within UHPC-CA. It was found that incorporating coarse aggregates (up to 30% by volume) enhanced the compressive strength of UHPC-CA at both room and elevated temperatures [116]. Post-fire curing of UHPC-CA, particularly in water environments, demonstrated substantial improvements in mechanical properties and permeability, with strength recovery rates exceeding 50% [105]. Lu et al. [117] developed a lightweight ultra-high-performance concrete (L-UHPC) with a density below 1800 kg/m<sup>3</sup> and a compressive strength exceeding 150 MPa. Incorporating high-strength hollow glass microspheres (HGM) and fine lightweight aggregates, L-UHPC attained remarkable material efficacy and mitigated the likelihood of explosive spalling. The integration of lightweight constituents and dry heat curing efficaciously diminished internal free water, augmenting fire resistance. Zhang and Tan [118] explored the conjoined effects of fine aggregate (FA) size, steel fiber, and PP fiber on the spalling characteristics and mechanical attributes of UHPC at elevated temperatures. The results demonstrated that the combination of PP fibers and large-sized FA significantly improved spalling resistance by augmenting permeability and reducing the requisite PP fiber quantity. In contrast, steel fibers and large-sized FA adversely affected mechanical properties above 600 °C. Microstructural examination revealed that the thermal expansion of steel fibers and aggregates severely damaged UHPC at elevated temperatures, while PP fibers enhanced permeability and spalling resistance via microcrack formation.

Quartz sand, river sand, or basalt are often used as conventional aggregates in UHPC, which, in addition to causing irreversible damage to the natural environment and human health, also have a certain disposal cost, so it is important to find healthy, environmentally friendly, and sustainable alternatives to these materials [119]. Ali H. AlAteah [120] assessed the incorporation of geranium plant waste (GP) and waste glass powder (WG) into ultra-high performance basalt fiber concrete (UHPBFC) to enhance its mechanical properties and sustainability. Lyu's group [121,122] explored the impact of incorporating crumb rubber (CR) into UHPC exposed to elevated temperatures.

The findings indicated that CR effectively mitigated the risk of spalling in UHPC, particularly at 600 °C. The inclusion of CR enhanced the material's microstructural properties by increasing pore connectivity, which facilitated the escape of vapor and reduced internal pressure. Additionally, the compressive strength of UHPC increased at 300 °C but decreased at 600 °C. This research highlighted the potential of using CR from waste tires in sustainable construction, offering valuable insights for future studies on UHPC's performance under high-temperature conditions.

In summary, while searching for low-cost, eco-friendly, or recyclable substances to replace traditional aggregates, it is imperative to not only improve the mechanical behavior of UHPC itself but also strive to make a contribution to the fire resistance.

### 3.4. Size of dimension

Most experiments have small specimen sizes, as shown in Table S2 in Supporting information. Nevertheless, there is a paucity of knowledge on the size effect on structural members made of UHPC [19]. Only a small number of investigations have been carried out on UHPC beams subjected to fire. It should be emphasized that the specimen sizes in the existing studies are small, and the large-scale testing of full-size UHPC structures is required before practical application. Banerji et al. [123] conducted fire experiments on five large-sized UHPFRC beams with different fitment ratios. It was found that in UHPFRC beams, fire-induced spalling occurred primarily in the upper portion of the beams (compression zone), which stands in contrast to the NSC and HSC beams, where most of the spalling was localized on the fire-exposed bottom face and bottom corners. This spalling behavior in the compression zone led to a more rapid temperature increase in the compression region within the concrete, including the compression reinforcement. Apart from this, the addition of polypropylene fibers to UHPFRC substantially decreases the severity of fire-induced spalling of UHPFRC beams. Hou et al. [124] compared the performance of NSC and RPC simply supported beams under fire and found that the fire resistance of RPC beams was lower than that of NSC beams under the same bending capacity and section conditions. To improve the fire resistance of RPC beams, it is necessary to take fire protection measures or increase the longitudinal reinforcement.

A number of applications of UHPC in flat components are listed in Section 2, however, UHPC either as a structural or non-structural system is susceptible to high temperatures in some scenarios. In addition, slabs/panels differ from beams/column in that the depth of the slab and the restraining effect of the reinforcement mesh have a significant impact on the pore pressure at high temperatures [125]. Zhang et al. [126] examined the fire resistance of ultra-high-performance polypropylene fiber reinforced concrete (UHPPFRC) panels using a coupled hygro-thermal-mechanical model. The research demonstrated that the inclusion of PP fibers significantly improved the fire resistance of UHPPFRC by enhancing pore pressure relief and reducing thermal stress. The tensile strength of the panels varied with fiber orientation, and the model accurately predicted internal stress and temperature distribution. The findings suggested that a 0.55% dosage of PP fiber effectively delayed crack propagation, highlighting the potential of PP fibers in improving the fire performance and durability of UHPPFRC panels. In a study exploring the thermal behaviors of FGC slabs under fire, Du et al. [40] designed two-layered slabs integrating UHPC for structural strength and LWAC for insulation. Fire resistance tests revealed that LWAC effectively reduced temperature transfer to UHPC layers, preventing explosive spalling and maintaining structural integrity. The research suggested an optimal LWAC layer thickness between 30–40 mm, providing a balance between thermal insulation and structural performance in fire scenarios. Moreover, the interface between LWAC and UHPC

maintained excellent bonding properties and superior stability after exposure to the ISO-834 heating curve for two hours [127].

This approach offers a promising direction for enhancing the fire resistance of reinforced concrete structures. However, research on UHPC slabs/panels at elevated temperatures is quite scarce and inadequate to support the development of UHPC design guidelines. In addition to the requirement to improve the spalling resistance of UHPC, attention needs to be paid to aspects such as crack extension, fiber orientation and post-damage properties.

### 3.5. *Cooling method*

The common cooling methods for concrete experiments are natural cooling (air cooling) or water cooling, and researchers have compared the effects of air-cooling and water-cooling on concrete after exposure to high temperatures. Wang et al. [128] showed experimentally that the compressive and splitting tensile capacities of concrete decreased with elevated temperatures after both natural and water cooling. The residual compressive and tensile strengths of concrete under water cooling were not as good as those under natural cooling since the cracks produced on the surface of the specimens cooled in water were more numerous and wider than those of the naturally cooled specimens. Kara's [129] results showed that the mass loss of concrete increased, and ultrasonic pulse velocity and compressive strength decreased as the temperature increased. The compressive strength of concrete was reduced by 71% and 61% at 700 °C for air cooling and water cooling, respectively. Awal et al. [130] reported that water-cooled concrete had less mass reduction but more strength reduction than air-cooled concrete. Durgun et al. [131] observed that water-cooled concrete was stronger than air-cooled concrete at 200–600 °C, but the opposite was true at 800 and 1000 °C. Fehérvári [132] examined five cooling methods and found that slow cooling rates resulted in higher strength, but the cooling methods did not have much impact on the high-temperature concrete in general.

Research on the effect of certain high-temperature cooling methods on the UHPC of fireproof coatings has not been reported, and whether fireproof coatings can perform the role of protecting the UHPC during water cooling deserves exploration. If the experimental conditions permit, the investigation of large-size UHPC members is more in line with practical engineering requirements.

### 3.6. *External load and restraint*

It was observed that the UHPC structural beams presented a lower degree of spalling at higher load levels, which was attributed to an increase in cracking in the tensile zone of the beams and a reduction in pore pressure [123]. Similarly, Qin et al. [133] showed that load ratio had a significant effect on the fire resistance of UHPC beams. As the load ratio increased, the failure time of the beams in a fire was drastically reduced, resulting in the development of microcracks in the beams and the formation of open joint channels between the internal holes. This phenomenon facilitated the release of vapor pressure and had a positive effect on reducing the extent of spalling. According to Yang et al. [134], the UHPC beams with the same ratio of shear span to effective depth displayed a different shear damage pattern at elevated temperatures than at ambient temperatures. In addition, the fire resistance remarkably increased with decreasing load ratio and shear span to effective depth ratio. The higher longitudinal reinforcement ratios and stirrup ratios were beneficial in resisting crack development and mitigating shear damage embrittlement. Ren et al. [135] discovered that current



design approaches could not offer a satisfactory assessment of the fire resistance of hybrid fiber-reinforced RPC beams. Hence, the existing macroscopic finite element model was broadened to mimic the fire behavior of such beams through extensive parametric exploration. Subsequently, a particular fire resistance standard was suggested to avert brittle failure caused by inadequate reinforcement during a fire, contributing to the improvement of UHPC design guidelines.

In terrible and complex fire environments, concrete might not only be subjected to static loads but also to dynamic loads, such as explosions and the impact of falling objects. Therefore, it is crucial to investigate the mechanical properties of UHPC under static or impact loads at different high temperatures. Most of the past research on the mechanical properties of UHPC at elevated temperatures has been conducted under static loading. However, few studies have been reported on impact loading, and the exploration of UHPC components with fire insulation has just started. In addition, the UHPC members in most of the studies are not sufficient to cover practical applications, and other restraints deserve to be investigated.

## **4. Approaches for mitigating fire-induced spalling**

### *4.1. Fire insulation*

The fireproof coating, with its low thermal conductivity, impedes the direct heat transfer from external heat sources to the internal structure. This decelerates the rate of structural heating, extends the time for structural degradation, and elevates the fire resistance limit of the structure [136]. Applying fireproof coatings can cut down on both the economic losses from fires and the subsequent maintenance costs. Consequently, scholars have carried out experimental research on the performance of concrete with fireproof coatings under high temperatures. Two types of fireproofing coatings are commonly used: intumescent and non-intumescent. Intumescent fireproof coating (IFC) expands to insulate against heat when exposed to fire, while non-intumescent fireproof coating (NIFC) relies on its own thickness and material properties to insulate. The test results of Hou et al. [137] showed that IFC can significantly reduce spalling, bursting, and cracking of concrete and effectively prevent the concrete structure from reaching very high temperatures. In addition, the deflection of prestressed concrete structures at high temperatures was greatly decreased, effectively protecting the structural prestressing. Ma et al. [136] discussed the various factors affecting the insulating, flaking, and residual properties of cementitious materials, a non-intumescent fireproofing coating, and summarized the different theories involved. It can be concluded that cement-based materials possess outstanding thermal insulation capabilities, anti-spalling characteristics, and enhanced mechanical properties following exposure to elevated temperatures. These enhanced properties are achieved by incorporating inorganic porous fillers, short fibers, and calcined products into the material composition. Mathews et al. [138] studied the fire response efficiency and the residual capacity of short columns of self-compacting concrete (SCC) with different protective coatings. The results revealed that specimens protected by cement perlite plaster (CPP) achieved the best protection against heat penetration and could be used as a protective interface for structural elements to minimize the effects of exposure to higher temperatures in fire incidents.

Based on the above research status, it can be seen that some types of fireproofing coatings have been proven to improve the fire performance of structures. However, research on fire protection coatings and UHPC is quite limited, and the capability of fire protection coatings to mitigate the

spalling of UHPC at elevated temperatures deserves further study. Hou et al.'s [139] research team tested four hybrid fiber-reinforced reactive powder concrete (RPC) beams that were protected by fireproof insulation and exposed to fire. The results showed that the damage to the RPC beams with fire insulation was caused by direct fire exposure and longitudinal reinforcement breakage after the collapse of the fire insulation, as well as the development of wide cracks in the beams. In this regard, the simultaneous use of hybrid fibers (2% steel fibers and 0.2% PP fibers) and fireproof insulation is an effective method to prevent fire spalling of reinforced RPC beams, which can significantly improve the fire resistance of hybrid fiber-reinforced RPC beams. In addition, Hou et al.'s team [140] developed a three-dimensional sequentially coupled heat-stress finite element model with software ABAQUS to simulate the behavior of insulated reinforced RPC beams under fire. The simulation results were compared with fire test results to verify their reliability. By varying the input parameters for the study, the thermal conductivity, thickness, mode of setting and height of the fireproofing insulation exhibited a greater influence on the fire resistance of the insulated and reinforced RPC beams, but the density and specific heat had a lesser effect on their fire resistance.

Limited and inadequate research cannot fully explain the effect of fire insulation on the fire performance of UHPC, nor can it support the development of fire design guidelines for UHPC, e.g., changes in the internal mechanisms of UHPC materials with different types of fire insulation at elevated temperatures, and the effectiveness of fire insulation on UHPC laminates, etc., are unknown.

#### 4.2. Curing method

The curing regime is also considered to be one of the effective ways to prevent explosive spalling, and the effect of various curing regimes on fire-induced explosive spalling is under continuous investigation. The effect of temperature on the mechanical and spalling behavior of UHPC under water curing was investigated by Kahanji et al. [141]. Two steel fiber-reinforced beams cured in cold (20 °C) and hot (90 °C) water, respectively, were placed in the fire and subjected to no-load tests. Both beams showed significant spalling, especially the beam cured with hot water. This is mainly because UHPC cured in hot water at 90 °C forms a denser microstructure, which prevents the escape of vapor. High temperature is a critical factor in achieving ultra-high strength of UHPC, and moisture content is a crucial parameter in determining the probability of spalling of UHPC [115,142]. Yan's research group [143] evaluated the fire exposure behavior of full-size prestressed RPC beams using hot-air curing. It was found that 150 °C hot-air curing could be a promising method to prevent RPC fire-induced spalling and enhance RPC strength in the short term. The explanation for this is that the 150 °C temperature can remarkably reduce the vapor pressure effect by accelerating the escape of evaporated free water. The 150 °C temperature can also raise the tensile strength of RPC to resist thermal stresses by promoting cement hydration and pozzolanic reaction. Therefore, a new curing regime, two-stage hot air curing (THAC), was proposed, as shown in Table 4, and it was proved that almost all the free water of UHPC cured by THAC could be consumed and evaporated, which greatly improved the anti-explosive spalling property of UHPC [133]. THAC could almost completely prevent the occurrence of UHPC of different sizes and different stress states from fire-induced explosion spalling and enhance its mechanical performance. Additionally, it has been shown that the tensile strength of RPC increases after high temperatures of 200~300 °C compared to steam curing, and the fire spalling of RPC can be prevented due to the lower water content of RPC [144]. Peng et al. [145] experimentally investigated the effect of hot water pre-curing and combined curing with dry air heating

at 200 or 250 °C on the spalling behavior of UHPC. The results showed that the combined curing exhibited two advantages: (i) it could significantly improve the mechanical properties of UHPC, and the effect was more efficient with the longer dry-air-heat curing time and the higher temperature; and (ii) it could significantly boost the explosive spalling resistance of UHPC at elevated temperatures due to the internal free-water minimization mechanism. It is worth noting that the effect of the above curing regimes on the behavior of large-sized UHPC components under fire is understudied and requires further research.

**Table 4.** Details of different curing regimes.

Curing regimes	Curing details	Ref.
Standard curing	Curing at 20 °C in the air with a humidity of 95% for 28 days.	[133]
20 °C water curing	Water curing at 20 °C for 28 days.	[133]
90 °C hot water curing	Water curing at 90 °C for 48 h.	[133]
Dry air heating	200~300 °C dry air heating for 2 days	[144]
Steam curing	Steam curing at 90 °C for 48 h.	[133]
Two-stage hot air curing	Curing in 95% humid hot air at 50 °C for 24 hours + curing in hot air at 90/120/150/250 °C for another 24 h.	[133]
Combined curing	Pre-curing in 90 °C hot water for 2 days + heating in 200 or 250 °C dry air for 1 to 3 days.	[145]

#### 4.3. Addition of fibers or aggregates

Further studies are needed on the mechanisms and theories of the influence of different fibers or aggregates on the fire performance and mechanical properties of UHPC. Past research has tested the effect of many types or shapes of fibers on the behavior of UHPC spalling, e.g., steel fiber, PP fiber, PVA fiber, PE fiber, PA fiber, nylon fiber, jute fiber, carbon fiber, basalt fiber, synergistic flame-retardant polymer fiber, etc. The impact of steel fiber and synthetic polymer fiber on ultra-high-performance concrete at high temperatures has been the subject of numerous investigations. Nonetheless, in response to the demand for green and low-carbon materials, research into natural or recycled fibers that are both ecologically friendly and capable of successfully reducing fire-caused spalling should proceed. However, the same dosage of natural fibers cannot achieve the full spalling prevention effectiveness of polymer fibers [146]. Increasing the dosage of natural fibers in UHPC can also significantly impair their mechanical strength and underlying durability. In addition, the morphology, size, and critical dosage of the fibers also have a considerable impact on the anti-spalling properties of UHPC, and the ultra-short fiber or polymers in granular form that can be uniformly distributed in the matrix also deserve to be an object of consideration.

Researchers have explored the role of different types and particle sizes of aggregates on the spalling behavior of UHPC, basalt aggregate, bauxite aggregate, steel slag, crushed dolomite, waste glass, etc. Other low-carbon, sustainable, and eco-friendly aggregates deserve to be further investigated.

#### 4.4. Thermal spalling-resistant admixtures

A type of addition of spalling-resistant admixtures can improve the pore structure and decrease the porosity of the concrete. This results in denser particle packing and reduces the amount of air as well as moisture residue within the material. The incorporation of nano-clay [147] and nano-silica [148], for example, increases the potential for thermal resistance while enhancing the mechanical properties of UHPC. Moreover, the addition of high-strength hollow microspheres as additives not only lightens the self-weight of UHPC but also considerably mitigates the spalling behavior [117]. The microstructural results showed that the voids created by the heat-collapsed glass microspheres could release some internal vapor pressure. The principle is similar to the use of air-entraining agents to prepare concrete mixtures with the introduction of small air voids, with voids favorable for accommodating water and enhancing the permeability of the concrete [149]. However, this method can significantly degrade the mechanical properties of UHPC. Therefore, it is urgent and revolutionary to search for additives that can balance the efficiency of UHPC materials with spalling prevention performance.

### 5. Conclusions and recommendations

The utilization of UHPC is becoming increasingly prevalent in the construction of flat components, attributed to its remarkable material properties. When combined with materials such as steel, wood, and conventional concrete, UHPC not only minimizes the consumption of resources but also enhances the structural performance, allowing for tailored applications in various construction projects. The roles UHPC plays in construction can be broadly classified into protection, rehabilitation, and reinforcement. These functions are largely dictated by the thickness of the UHPC layer and its interaction with steel reinforcement.

However, UHPC presents a significant challenge under fire conditions due to its susceptibility to explosive spalling. If not adequately addressed, this vulnerability can lead to the premature failure of UHPC structures when exposed to high temperatures. Researchers have identified pore pressure and thermal stresses as primary contributors to this phenomenon, with existing models attempting to elucidate these mechanisms. However, these models may not fully capture the complexity of the spalling process.

The integration of polymer synthetic fibers has shown promise in mitigating explosive spalling by facilitating the release of vapor pressure. Fibers such as polypropylene, nylon, polyvinyl alcohol, and linear low-density polyethylene fibers have demonstrated beneficial effects, independent of their melting points. Notably, a hybrid approach using PP and steel fibers enhances the spalling resistance, with the content and aspect ratio of PP fibers being critical parameters. The sole effectiveness of steel fibers remains contentious. Additionally, incorporating aggregates like hollow glass microspheres or crumb rubber, which disintegrate or melt upon heating, further mitigates spalling by alleviating internal vapor pressure.

Moreover, dry-air-heat curing emerges as a potent method to diminish vapor pressure effects by expediting the escape of evaporated moisture, thereby significantly bolstering UHPC's resistance to explosive spalling at elevated temperatures. The application of fireproof coatings and refractory insulation materials also contributes to reducing the heat-up rate, mitigating spalling induced by severe thermal gradients. These strategies collectively represent a multifaceted approach to enhancing the fire resistance of UHPC, ensuring its structural integrity and longevity in fire-prone environments.

Although UHPC exhibits excellent mechanical properties and the potential for application in different scenarios, its application and promotion require more attention to investigation due to its high material cost and vulnerability to fire exposure. The limitations of this study and recommendations for the future are summarized below:

- Feasibility validation: the application of UHPC in flat components is in its early stages, and the feasibility of different applications in practical engineering needs further validation and optimization.
- Creative applications: the development of creative flat component applications should be pursued by combining UHPC with other materials or structures to take full advantage of the strengths and benefits of UHPC performance and to reduce consumption.
- Interface performance: the interfacial connections, bonding behavior, or interactions are usually prone to serve as weak areas when UHPC acts in conjunction with other materials. Therefore, interfacial performance should also be an important aspect of composite structures that deserves attention and continued research.
- Standards and codes: the current standards and codes for UHPC flat components and fire design requirements do not take into account the risk of fire-induced spalling that can occur in concrete structures. This is a significant shortcoming of the design guidelines and hinders the promotion of UHPC in building structures.
- Mechanism and prediction models: an in-depth understanding of the complex spalling mechanism of UHPC is difficult, and more sophisticated and comprehensive numerical prediction models are needed to accurately simulate the physical and chemical properties of UHPC under high temperatures.
- Different types of fibers: several studies have examined the impact of steel and polymer synthetic fibers on UHPC at high temperatures. However, there is a need for further research on the utilization of natural or recycled fibers that are both eco-friendly and effective in reducing fire-induced spalling.
- Scale effect: most of the studies were conducted on small-scale specimens. Some studies tested large-size beams and columns on fire, but very few investigations have been done on large-size UHPC slabs.
- Innovative improvement solutions: in addition to some measures of improvement at the material level, such as fiber or aggregate additions, other innovative solutions need to be urgently explored to improve the behavior of UHPC flat components at elevated temperatures.

## Use of AI tools declaration

The authors declare they have not used Artificial Intelligence (AI) tools in the creation of this article.

## Acknowledgment

The authors would like to acknowledge the support of Xi'an Jiaotong-Liverpool University for providing the necessary resources used in carrying out this review work.

## Author contributions

Xiaodong Cheng: writing—review & editing, writing—original draft, visualization, methodology, investigation, data curation, conceptualization. Jun Xia: writing—review & editing, visualization, supervision, methodology, investigation, conceptualization. Theofanis Krevaiakas: writing—review &

editing, supervision, methodology, investigation. Luigi Di Sarno: writing—review & editing, supervision, methodology, investigation.

## Conflict of interest

The authors declare no conflict of interest.

## References

1. Xiao J, Xie Q, Xie W (2018) Study on high-performance concrete at high temperatures in China (2004–2016)-An updated overview. *Fire Safety J* 95: 11–24. <https://doi.org/10.1016/j.firesaf.2017.10.007>
2. Abid M, Hou X, Zheng W, et al. (2017) High temperature and residual properties of reactive powder concrete—A review. *Constr Build Mater* 147: 339–351. <https://doi.org/10.1016/j.conbuildmat.2017.04.083>
3. Wen C, Zhang P, Wang J, et al. (2022) Influence of fibers on the mechanical properties and durability of ultra-high-performance concrete: A review. *J Build Eng* 52: 104370. <https://doi.org/10.1016/j.job.2022.104370>
4. Yoo DY, Yoon YS (2016) A review on structural behavior, design, and application of ultra-high-performance fiber-reinforced concrete. *Int J Concr Struct Mater* 10: 125–142. <https://doi.org/10.1007/s40069-016-0143-x>
5. Shaikh FUA, Luhar S, Arel HŞ, et al. (2020) Performance evaluation of ultrahigh performance fibre reinforced concrete—A review. *Constr Build Mater* 232: 117152. <https://doi.org/10.1016/j.conbuildmat.2019.117152>
6. Zhu Y, Zhang Y, Hussein HH, et al. (2020) Flexural strengthening of reinforced concrete beams or slabs using ultra-high performance concrete (UHPC): A state of the art review. *Eng Struct* 205: 110035. <https://doi.org/10.1016/j.engstruct.2019.110035>
7. Haber ZB, Munoz JF, De la Varga I, et al. (2018) Bond characterization of UHPC overlays for concrete bridge decks: Laboratory and field testing. *Constr Build Mater* 190: 1056–1068. <https://doi.org/10.1016/j.conbuildmat.2018.09.167>
8. Rambabu D, Sharma SK, Karthik P, et al. (2023) A review of application of UHPFRC in bridges as an overlay. *Innov Infrastruct Solut* 8: 57. <https://doi.org/10.1007/s41062-022-01030-4>
9. Kadhim MMA, Saleh AR, Cunningham LS, et al. (2021) Numerical investigation of non-shear-reinforced UHPC hybrid flat slabs subject to punching shear. *Eng Struct* 241: 112444. <https://doi.org/10.1016/j.engstruct.2021.112444>
10. Lamothe S, Sorelli L, Blanchet P, et al. (2020) Engineering ductile notch connections for composite floors made of laminated timber and high or ultra-high performance fiber reinforced concrete. *Eng Struct* 211: 110415. <https://doi.org/10.1016/j.engstruct.2020.110415>
11. Lamothe S, Sorelli L, Blanchet P, et al. (2021) Lightweight and slender timber-concrete composite floors made of CLT-HPC and CLT-UHPC with ductile notch connectors. *Eng Struct* 243: 112409. <https://doi.org/10.1016/j.engstruct.2021.112409>
12. Xue J, Briseghella B, Huang F, et al. (2020) Review of ultra-high performance concrete and its application in bridge engineering. *Constr Build Mater* 260: 119844. <https://doi.org/10.1016/j.conbuildmat.2020.119844>

13. Hung CC, El-Tawil S, Chao SH (2021) A review of developments and challenges for UHPC in structural engineering: Behavior, analysis, and design. *J Struct Eng* 147: 03121001. [https://doi.org/10.1061/\(ASCE\)ST.1943-541X.0003073](https://doi.org/10.1061/(ASCE)ST.1943-541X.0003073)
14. Pharand M, Charron JP (2023) Prediction of moment–curvature response and maximum bending resistance for hybrid NSC-UHPC elements. *J Struct Eng* 149: 04023162. <https://doi.org/10.1061/JSENDH.STENG-12407>
15. Amran M, Huang SS, Onaizi AM, et al. (2022) Recent trends in ultra-high performance concrete (UHPC): Current status, challenges, and future prospects. *Constr Build Mater* 352: 129029. <https://doi.org/10.1016/j.conbuildmat.2022.129029>
16. Iso I (1999) Fire resistance tests-elements of building construction. International Organization for Standardization, Geneva, Switzerland.
17. Choe G, Kim G, Gucunski N, et al. (2015) Evaluation of the mechanical properties of 200 MPa ultra-high-strength concrete at elevated temperatures and residual strength of column. *Constr Build Mater* 86: 159–168. <https://doi.org/10.1016/j.conbuildmat.2015.03.074>
18. Li X, Bao Y, Wu L, et al. (2017) Thermal and mechanical properties of high-performance fiber-reinforced cementitious composites after exposure to high temperatures. *Constr Build Mater* 157: 829–838. <https://doi.org/10.1016/j.conbuildmat.2017.09.125>
19. Amran M, Murali G, Makul N, et al. (2023) Fire-induced spalling of ultra-high performance concrete: A systematic critical review. *Constr Build Mater* 373: 130869. <https://doi.org/10.1016/j.conbuildmat.2023.130869>
20. Kodur V, Banerji S (2021) Modeling the fire-induced spalling in concrete structures incorporating hydro-thermo-mechanical stresses. *Cem Concr Compos* 117: 103902. <https://doi.org/10.1016/j.cemconcomp.2020.103902>
21. Nassar RUD, Zaid O, Althoey F, et al. (2024) Spalling behavior and performance of ultra-high-performance concrete subjected to elevated temperature: A review. *Constr Build Mater* 411: 134489. <https://doi.org/10.1016/j.conbuildmat.2023.134489>
22. Zhu Y, Hussein H, Kumar A, et al. (2021) A review: Material and structural properties of UHPC at elevated temperatures or fire conditions. *Cem Concr Compos* 123: 104212. <https://doi.org/10.1016/j.cemconcomp.2021.104212>
23. Aaleti S, Sritharan S (2019) Quantifying bonding characteristics between UHPC and normal-strength concrete for bridge deck application. *J Bridge Eng* 24: 04019041. [https://doi.org/10.1061/\(ASCE\)BE.1943-5592.0001404](https://doi.org/10.1061/(ASCE)BE.1943-5592.0001404)
24. Deng P, Mi H, Mitamura H, et al. (2022) Stress reduction effects of ultra-high performance fiber reinforced concrete overlaid steel bridge deck developed with a new interfacial bond method. *Constr Build Mater* 328: 127104. <https://doi.org/10.1016/j.conbuildmat.2022.127104>
25. Wei Y, Guo W, Ma L, et al. (2023) Materials, structure, and construction of a low-shrinkage UHPC overlay on concrete bridge deck. *Constr Build Mater* 406: 133353. <https://doi.org/10.1016/j.conbuildmat.2023.133353>
26. Zhu Y, Zhang Y, Hussein HH, et al. (2022) Flexural strengthening of large-scale damaged reinforced concrete bridge slab using UHPC layer with different interface techniques. *Struct Infrastruct Eng* 18: 879–892. <https://doi.org/10.1080/15732479.2021.1876104>
27. Wei C, Zhang Q, Yang Z, et al. (2022) Flexural cracking behavior of reinforced UHPC overlay in composite bridge deck with orthotropic steel deck under static and fatigue loads. *Eng Struct* 265: 114537. <https://doi.org/10.1016/j.engstruct.2022.114537>



28. Walter R, Olesen JF, Stang H, et al. (2007) Analysis of an orthotropic deck stiffened with a cement-based overlay. *J Bridge Eng* 12: 350–363. [https://doi.org/10.1061/\(ASCE\)1084-0702\(2007\)12:3\(350\)](https://doi.org/10.1061/(ASCE)1084-0702(2007)12:3(350))
29. Tan C, Luo Z, Zhao H, et al. (2023) Flexural Behavior on a steel–UHPC composite deck system of long-span bridges. *J Bridge Eng* 28: 04023062. <https://doi.org/10.1061/JBENF2.BEENG-6323>
30. Tan X, Fang Z, Wu X, et al. (2024) Flexural performance of a prefabricated steel–UHPC composite deck under transverse hogging moment. *Eng Struct* 305: 117783. <https://doi.org/10.1016/j.engstruct.2024.117783>
31. Sun B, Xiao R, Song C, et al. (2022) Design and experimental study of a replaceable steel-UHPC composite bridge deck. *Structures* 40: 1107–1120. <https://doi.org/10.1016/j.istruc.2022.04.091>
32. Bu Y, Li M, Wei C, et al. (2023) Experimental and analytical studies on flexural behavior of composite bridge decks with orthotropic steel deck and ultra-high-performance concrete (UHPC) slab under negative moment. *Eng Struct* 274: 115190. <https://doi.org/10.1016/j.engstruct.2022>
33. Ma CH, Deng P, Matsumoto T (2021) Fatigue analysis of a UHPFRC-OSD composite structure considering crack bridging and interfacial bond stiffness degradations. *Eng Struct* 249: 113330. <https://doi.org/10.1016/j.engstruct.2021.113330>
34. Naud N, Sorelli L, Salenikov A, et al. (2019) Fostering GLULAM-UHPFRC composite structures for multi-storey buildings. *Eng Struct* 188: 406–417. <https://doi.org/10.1016/j.engstruct.2019.02.049>
35. Nguyen TT, Sorelli L, Blanchet P (2023) Composite slab floors made of cross laminated timber and ultra high-performance concrete: Early-age deflection, stripping time, and its implication on the structural performances. *Eng Struct* 295: 116810. <https://doi.org/10.1016/j.engstruct.2023.116810>
36. Zohrevand P, Yang X, Jiao X, et al. (2015) Punching shear enhancement of flat slabs with partial use of ultrahigh-performance concrete. *J Mater Civil Eng* 27: 04014255. [https://doi.org/doi:10.1061/\(ASCE\)MT.1943-5533.0001219](https://doi.org/doi:10.1061/(ASCE)MT.1943-5533.0001219)
37. Qi J, Cheng Z, Zhou K, et al. (2021) Experimental and theoretical investigations of UHPC-NC composite slabs subjected to punching shear-flexural failure. *J Build Eng* 44: 102662. <https://doi.org/10.1016/j.jobe.2021.102662>
38. Zhou K, Qi J, Wang J (2023) Post-cracking punching shear behavior of concrete flat slabs partially reinforced with full-depth UHPC: Experiment and mechanical model. *Eng Struct* 275: 115313. <https://doi.org/10.1016/j.engstruct.2022.115313>
39. Torelli G, Fernández MG, Lees JM (2020) Functionally graded concrete: Design objectives, production techniques and analysis methods for layered and continuously graded elements. *Constr Build Mater* 242: 118040. <https://doi.org/10.1016/j.conbuildmat.2020.118040>
40. Du L, Ji X, Wang Y, et al. (2023) Experimental study on thermal behaviors of two-layered functionally graded concrete slabs subjected to fire. *Eng Struct* 297: 117047. <https://doi.org/10.1016/j.engstruct.2023.117047>
41. Du L, Ji X, Lu K, et al. (2023) Evaluation of bond behaviors on functionally graded ultra-high performance concrete (FGUHPC) subjected to elevated temperature. *Eng Struct* 274: 115112. <https://doi.org/10.1016/j.engstruct.2022.115112>
42. Yan B, Qiu M, Zeng T, et al. (2020) Full-scale experimental verification of UHPC-RC composite slab culvert with a clear span of 8 m. *J Bridge Eng* 25: 05020010. [https://doi.org/10.1061/\(asce\)be.1943-5592.0001640](https://doi.org/10.1061/(asce)be.1943-5592.0001640)

43. Guo W, Wei Y, Ma L (2022) Shrinkage-induced warping of UHPC overlay cast on hardened NSC substrate under various conditions. *Cement Concrete Comp* 134: 104772. <https://doi.org/10.1016/j.cemconcomp.2022.104772>
44. Guo W, Wei Y, Ma L, et al. (2023) Effect of grouped L-shape rebar connectors on the shrinkage behavior of UHPC overlay cast on hardened NSC substrate. *Constr Build Mater* 382: 131319. <https://doi.org/10.1016/j.conbuildmat.2023.131319>
45. Liu Y, Wei Y, Ma L, et al. (2022) Restrained shrinkage behavior of internally-cured UHPC using calcined bauxite aggregate in the ring test and UHPC-concrete composite slab. *Cem Concr Compos* 134: 104805. <https://doi.org/10.1016/j.cemconcomp.2022.104805>
46. Wang K, Zhao C, Wu B, et al. (2019) Fully-scale test and analysis of fully dry-connected prefabricated steel-UHPC composite beam under hogging moments. *Eng Struct* 197: 109380. <https://doi.org/10.1016/j.engstruct.2019.109380>
47. Wang J, Qi J, Tong T, et al. (2019) Static behavior of large stud shear connectors in steel-UHPC composite structures. *Eng Struct* 178: 534–542. <https://doi.org/10.1016/j.engstruct.2018.07.058>
48. Zhang Y, Zhu J, Wu L, et al. (2024) Experimental and numerical analyses on the shear behavior of grouped single-embedded-nut high-strength bolts in steel-ultra-high-performance concrete composite slabs. *J Build Eng* 86: 108829. <https://doi.org/10.1016/j.jobbe.2024.108829>
49. Xu Q, Sebastian W, Wang J (2024) Flexural performance of ultrathin UHPC slab–steel composite beams with ultrashort stud connections. *J Bridge Eng* 29: 04024022. <https://doi.org/doi:10.1061/JBENF2.BEENG-6492>
50. Xu Q, Sebastian W, Lu K, et al. (2022) Parametric experimental study of ultra-short stud connections for lightweight steel–UHPC composite bridges. *J Bridge Eng* 27: 04021108. [https://doi.org/10.1061/\(ASCE\)BE.1943-5592.0001821](https://doi.org/10.1061/(ASCE)BE.1943-5592.0001821)
51. Xu Q, Lu K, Wang J, et al. (2021) Performance of large-diameter studs in thin ultra-high performance concrete slab. *Structures* 34: 4936–4951. <https://doi.org/10.1016/j.istruc.2021.10.076>
52. Xu Q, Sebastian W, Lu K, et al. (2022) Longitudinal shear performance of lightweight steel-UHPC composite connections based on large-diameter high strength friction-grip bolts. *Eng Struct* 260: 114220. <https://doi.org/10.1016/j.engstruct.2022.114220>
53. Xu Q, Sebastian W, Lu K, et al. (2022) Development and performance of innovative steel wedge block–crossed inclined stud–UHPC connections for composite bridge. *J Struct Eng* 148: 04022128. [https://doi.org/10.1061/\(ASCE\)ST.1943-541X.0003437](https://doi.org/10.1061/(ASCE)ST.1943-541X.0003437)
54. Wang Z, Yan J, Lin Y, et al. (2020) Mechanical properties of steel-UHPC-steel slabs under concentrated loads considering composite action. *Eng Struct* 222: 111095. <https://doi.org/10.1016/j.engstruct.2020.111095>
55. Wang Z, Yan J, Lin Y, et al. (2021) Influence of shear connectors on the ultimate capacity of steel-UHPC-steel slabs subjected to concentrated loads. *Eng Struct* 231. <https://doi.org/10.1016/j.engstruct.2020.111763>
56. Wang Z, Yan J, Lin Y, et al. (2023) Experimental and analytical study on the double steel plates-UHPC sandwich slabs under low-velocity impact. *Thin Wall Struct* 184: 110548. <https://doi.org/10.1016/j.tws.2023.110548>
57. Wang Z, Yan J, Lin Y, et al. (2024) Impact response of SCS sandwich slabs with ultra-high performance concrete: Failure mechanism and influence of shear connector configuration. *Int J Impact Eng* 186: 104889. <https://doi.org/10.1016/j.ijimpeng.2024.104889>

58. Varma AH, Malushte SR, Sener KC, et al. (2014) Steel-plate composite (SC) walls for safety related nuclear facilities: Design for in-plane forces and out-of-plane moments. *Nucl Eng Des* 269: 240–249. <https://doi.org/10.1016/j.nucengdes.2013.09.019>
59. Lin M, Lin W, Wang Q, et al. (2018) The deployable element, a new closure joint construction method for immersed tunnel. *Tunn Undergr Sp Tech* 80: 290–300. <https://doi.org/10.1016/j.tust.2018.07.028>
60. Ji X, Cheng X, Jia X, et al. (2017) Cyclic in-plane shear behavior of double-skin composite walls in high-rise buildings. *J Struct Eng* 143: 04017025. [https://doi.org/10.1061/\(ASCE\)ST.1943-541X.0001749](https://doi.org/10.1061/(ASCE)ST.1943-541X.0001749)
61. Yan JB, Li ZX, Wang T (2018) Seismic behaviour of double skin composite shear walls with overlapped headed studs. *Constr Build Mater* 191: 590–607. <https://doi.org/10.1016/j.conbuildmat.2018.10.042>
62. Liew JR, Yan JB, Huang ZY (2017) Steel-concrete-steel sandwich composite structures-recent innovations. *J Constr Steel Res* 130: 202–221. <https://doi.org/10.1016/j.jcsr.2016.12.007>
63. Qiu M, Shao X, Yan B, et al. (2022) Flexural behavior of UHPC joints for precast UHPC deck slabs. *Eng Struct* 251: 113422. <https://doi.org/10.1016/j.engstruct.2021.113422>
64. Wang H, Zhou Z, Zhang Z, et al. (2023) Experimental and numerical studies on shear behavior of prefabricated bridge deck slabs with compact UHPC wet joint. *Case Stud Constr Mat* 19: e02362. <https://doi.org/10.1016/j.cscm.2023.e02362>
65. Hu M, Jia Z, Han Q, et al. (2022) Shear behavior of innovative high performance joints for precast concrete deck panels. *Eng Struct* 261: 114307. <https://doi.org/10.1016/j.engstruct.2022.114307>
66. Hu M, Jia Z, Han Q, et al. (2023) Experimental investigation of precast bridge deck panels with novel high-performance connections under fatigue loading. *J Bridge Eng* 28: 04023074. <https://doi.org/doi:10.1061/JBENF2.BEENG-6325>
67. Hu M, Jia Z, Xu L, et al. (2023) Flexural performance predictions of prefabricated bridge deck panels connected with CFRP tendons and UHPC grout. *Eng Struct* 285: 116024. <https://doi.org/10.1016/j.engstruct.2023.116024>
68. Qi J, Bao Y, Wang J, et al. (2019) Flexural behavior of an innovative dovetail UHPC joint in composite bridges under negative bending moment. *Eng Struct* 200: 109716. <https://doi.org/10.1016/j.engstruct.2019.109716>
69. Pharand M, Charron JP (2023) Experimental investigation of the shear resistance mechanism on hybrid NSC-UHPC predamaged and undamaged unidirectional bridge slabs. *J Struct Eng* 149: 04023128. <https://doi.org/10.1061/jsendh.Steng-12162>
70. Zhu Y, Zhang Y, Hussein HH, et al. (2020) Numerical modeling for damaged reinforced concrete slab strengthened by ultra-high performance concrete (UHPC) layer. *Eng Struct* 209: 110031. <https://doi.org/10.1016/j.engstruct.2019.110031>
71. Teng L, Khayat KH (2022) Effect of overlay thickness, fiber volume, and shrinkage mitigation on flexural behavior of thin bonded ultra-high-performance concrete overlay slab. *Cem Concr Compos* 134: 104752. <https://doi.org/10.1016/j.cemconcomp.2022.104752>
72. Kim S, Kang TH, Hong SG (2021) Impact performance of thin prefabricated ultra-high-performance concrete Façade. *ACI Struct J* 118: 167–177. <https://doi.org/10.14359/51728181>
73. Fabbri R, Corvez D (2013) Rationalisation of complex UHPFRC facade shapes. RILEM-*fib-AFGC International Symposium on Ultra-High Performance Fibre-Reinforced Concrete*, Marseille, France, 27–36.

74. Aubry S, Bompas P, Vaudeville B, et al. (2013) A UHPFRC cladding challenge: The fondation Louis Vuitton pour la création “Iceberg”. 2nd RILEM-*fib*-AFGC International Symposium on Ultra-High Performance Fibre-Reinforced Concrete, Marseille, France.
75. Menétrey P (2013) UHPFRC cladding for the Qatar National Museum. Proceedings of the International Symposium on Ultra-High Performance Fiber-Reinforced Concrete, Marseille, France.
76. Muttoni A, Brauen U, Jaquier JL, et al. (2013) A new roof for the olympic museum at Lausanne, Switzerland. Proceedings of International Symposium on Ultra-High Performance Fiber-Reinforced Concrete, Marseille, France, 69–76.
77. Delplace G, Hajar Z, Simon A, et al. (2013) Precast thin UHPFRC curved shells in a waste water treatment plant. Proceedings of the International Symposium on Ultra-High Performance Fiber-Reinforced Concrete, Marseille, France.
78. Azmee NM, Shafiq N (2018) Ultra-high performance concrete: From fundamental to applications. *Case Stud Constr Mat* 9: e00197. <https://doi.org/10.1016/j.cscm.2018.e00197>
79. Harsono K, Shih S, Chen Y (2023) The integration of design and fabrication for prefabricated UHPC panels of building facades. Proceedings of the 5th International Conference on Civil and Building Engineering Informatics, Bangkok, Thailand, 19–21.
80. Leone MF, Nocerino G (2021) Advanced modelling and digital manufacturing: Parametric design tools for the optimization of UHPFRC (ultra high-performance fiber reinforced concrete) shading panels. *Automat Constr* 126: 103650. <https://doi.org/10.1016/j.autcon.2021.103650>
81. Sayyafi EA, Chowdhury AG, Mirmiran A (2018) Innovative hurricane-resistant UHPC roof system. *J Archit Eng* 24: 04017032. [https://doi.org/10.1061/\(ASCE\)AE.1943-5568.0000290](https://doi.org/10.1061/(ASCE)AE.1943-5568.0000290)
82. Li Y, Tan KH, Yang EH (2019) Synergistic effects of hybrid polypropylene and steel fibers on explosive spalling prevention of ultra-high performance concrete at elevated temperature. *Cem Concr Compos* 96: 174–181. <https://doi.org/10.1016/j.cemconcomp.2018.11.009>
83. Zhang D, Dasari A, Tan KH (2018) On the mechanism of prevention of explosive spalling in ultra-high performance concrete with polymer fibers. *Cement Concrete Res* 113: 169–177. <https://doi.org/10.1016/j.cemconres.2018.08.012>
84. Debicki G, Haniche R, Delhomme F (2012) An experimental method for assessing the spalling sensitivity of concrete mixture submitted to high temperature. *Cem Concr Compos* 34: 958–963. <https://doi.org/10.1016/j.cemconcomp.2012.04.002>
85. Liu JC, Tan KH, Yao Y (2018) A new perspective on nature of fire-induced spalling in concrete. *Constr Build Mater* 184: 581–590. <https://doi.org/10.1016/j.conbuildmat.2018.06.204>
86. Xiao JZ, Meng XA, Zhang C (2006) Residual compressive behaviour of pre-heated high-performance concrete with blast-furnace-slag. *Fire Safety J* 41: 91–98. <https://doi.org/10.1016/j.firesaf.2005.11.001>
87. Xing Z, Beaucour AL, Hebert R, et al. (2011) Influence of the nature of aggregates on the behaviour of concrete subjected to elevated temperature. *Cement Concrete Res* 41: 392–402. <https://doi.org/10.1016/j.cemconres.2011.01.005>
88. Annerel E, Taerwe L (2009) Revealing the temperature history in concrete after fire exposure by microscopic analysis. *Cement Concrete Res* 39: 1239–1249. <https://doi.org/10.1016/j.cemconres.2009.08.017>

89. Li Y, Tan KH, Yang EH (2018) Influence of aggregate size and inclusion of polypropylene and steel fibers on the hot permeability of ultra-high performance concrete (UHPC) at elevated temperature. *Constr Build Mater* 169: 629–637. <https://doi.org/10.1016/j.conbuildmat.2018.01.105>
90. Ye G, Liu X, De Schutter G, et al. (2007) Phase distribution and microstructural changes of self-compacting cement paste at elevated temperature. *Cement Concrete Res* 37: 978–987. <https://doi.org/10.1016/j.cemconres.2007.02.011>
91. Khoury G (2008) Polypropylene fibres in heated concrete. Part 2: Pressure relief mechanisms and modelling criteria. *Mag Concrete Res* 60: 189–204. <https://doi.org/10.1680/macr.2007.00042>
92. Zhao J, Zheng JJ, Peng GF, et al. (2017) Numerical analysis of heating rate effect on spalling of high-performance concrete under high temperature conditions. *Constr Build Mater* 152: 456–466. <https://doi.org/10.1016/j.conbuildmat.2017.07.023>
93. Felicetti R, Lo Monte F, Pimienta P (2017) A new test method to study the influence of pore pressure on fracture behaviour of concrete during heating. *Cement Concrete Res* 94: 13–23. <https://doi.org/10.1016/j.cemconres.2017.01.002>
94. Liang XW, Wu CQ, Su Y, et al. (2018) Development of ultra-high performance concrete with high fire resistance. *Constr Build Mater* 179: 400–412. <https://doi.org/10.1016/j.conbuildmat.2018.05.241>
95. Liang XW, Wu CQ, Yang YK, et al. (2019) Experimental study on ultra-high performance concrete with high fire resistance under simultaneous effect of elevated temperature and impact loading. *Cem Concr Compos* 98: 29–38. <https://doi.org/10.1016/j.cemconcomp.2019.01.017>
96. Sciarretta F, Fava S, Francini M, et al. (2021) Ultra-high performance concrete (UHPC) with polypropylene (Pp) and steel fibres: Investigation on the high temperature behaviour. *Constr Build Mater* 304: 124608. <https://doi.org/10.1016/j.conbuildmat.2021.124608>
97. Viana TM, Bacelar BA, Coelho ID, et al. (2020) Behaviour of ultra-high performance concretes incorporating carbon nanotubes under thermal load. *Constr Build Mater* 263: 120556. <https://doi.org/10.1016/j.conbuildmat.2020.120556>
98. Zhang XY, Cai SH, Wang ZH, et al. (2022) Research on mechanical properties of ultra-high performance fiber reinforced cement-based composite after elevated temperature. *Compos Struct* 291: 115584. <https://doi.org/10.1016/j.compstruct.2022.115584>
99. Abid M, Hou XM, Zheng WZ, et al. (2017) High temperature and residual properties of reactive powder concrete—A review. *Constr Build Mater* 147: 339–351. <https://doi.org/10.1016/j.conbuildmat.2017.04.083>
100. Zheng WZ, Luo BF, Wang Y (2013) Compressive and tensile properties of reactive powder concrete with steel fibres at elevated temperatures. *Constr Build Mater* 41: 844–851. <https://doi.org/10.1016/j.conbuildmat.2012.12.066>
101. Shen Y, Dai M, Pu W, et al. (2022) Effects of content and length/diameter ratio of PP fiber on explosive spalling resistance of hybrid fiber-reinforced ultra-high-performance concrete. *J Build Eng* 58: 105071. <https://doi.org/10.1016/j.job.2022.105071>
102. Li Y, Pimienta P, Pinoteau N, et al. (2019) Effect of aggregate size and inclusion of polypropylene and steel fibers on explosive spalling and pore pressure in ultra-high-performance concrete (UHPC) at elevated temperature. *Cem Concr Compos* 99: 62–71. <https://doi.org/10.1016/j.cemconcomp.2019.02.016>

103. Zhang D, Tan KH (2022) Critical fiber dimensions for preventing spalling of ultra-high performance concrete at high temperature. *Fire Technol* 60: 3043–3058. <https://doi.org/10.1007/s10694-022-01318-y>
104. Huang L, Du Y, Zhu S, et al. (2023) Material property and constitutive model of C120 hybrid fiber ultra-high performance concrete at elevated temperatures. *Structures* 50: 373–386. <https://doi.org/10.1016/j.istruc.2023.02.057>
105. Qian Y, Yang D, Xia Y, et al. (2023) Properties and improvement of ultra-high performance concrete with coarse aggregates and polypropylene fibers after high-temperature damage. *Constr Build Mater* 364: 129925. <https://doi.org/10.1016/j.conbuildmat.2022.129925>
106. Ali M, Elsayed M, Tayeh BA, et al. (2024) Effect of hybrid steel, polypropylene, polyvinyl alcohol, and jute fibers on the properties of ultra-high performance fiber reinforced concrete exposed to elevated temperature. *Struct Concr* 25: 492–505. <https://doi.org/10.1002/suco.202300074>
107. Zhang D, Tan KH, Dasari A, et al. (2020) Effect of natural fibers on thermal spalling resistance of ultra-high performance concrete. *Cem Concr Compos* 109: 103512. <https://doi.org/10.1016/j.cemconcomp.2020.103512>
108. Missemer L, Ouedraogo E, Malecot Y, et al. (2019) Fire spalling of ultra-high performance concrete: From a global analysis to microstructure investigations. *Cement Concrete Res* 115: 207–219. <https://doi.org/10.1016/j.cemconres.2018.10.005>
109. Lee NK, Koh KT, Park SH, et al. (2017) Microstructural investigation of calcium aluminate cement-based ultra-high performance concrete (UHPC) exposed to high temperatures. *Cement Concrete Res* 102: 109–118. <https://doi.org/10.1016/j.cemconres.2017.09.004>
110. Zhang D, Chen B, Wu X, et al. (2022) Effect of polymer fibers on pore pressure development and explosive spalling of ultra-high performance concrete at elevated temperature. *Arch Civ Mech Eng* 22: 187. <https://doi.org/10.1007/s43452-022-00520-7>
111. Zhang T, Zhang M, Shen Y, et al. (2022) Mitigating the damage of ultra-high performance concrete at elevated temperatures using synergistic flame-retardant polymer fibres. *Cement Concrete Res* 158: 106835. <https://doi.org/10.1016/j.cemconres.2022.106835>
112. Park JJ, Yoo DY, Kim S, et al. (2019) Benefits of synthetic fibers on the residual mechanical performance of UHPFRC after exposure to ISO standard fire. *Cem Concr Compos* 104: 103401. <https://doi.org/10.1016/j.cemconcomp.2019.103401>
113. Cai R, Liu JC, Ye H (2021) Spalling prevention of ultrahigh-performance concrete: comparative effectiveness of polyethylene terephthalate and polypropylene fibers. *J Mater Civil Eng* 33: 04021344. [https://doi.org/10.1061/\(ASCE\)MT.1943-5533.0003980](https://doi.org/10.1061/(ASCE)MT.1943-5533.0003980)
114. Shi C, Wu Z, Xiao J, et al. (2015) A review on ultra high performance concrete: Part I. Raw materials and mixture design. *Constr Build Mater* 101: 741–751. <https://doi.org/10.1016/j.conbuildmat.2015.10.088>
115. Yang J, Peng GF, Zhao J, et al. (2019) On the explosive spalling behavior of ultra-high performance concrete with and without coarse aggregate exposed to high temperature. *Constr Build Mater* 226: 932–944. <https://doi.org/10.1016/j.conbuildmat.2019.07.299>
116. Xue C, Yu M, Xu H, et al. (2023) Compressive performance and deterioration mechanism of ultra-high performance concrete with coarse aggregates under and after heating. *J Build Eng* 64: 105502. <https://doi.org/10.1016/j.job.2022.105502>

117. Lu JX, Shen P, Sun Y, et al. (2022) Strategy for preventing explosive spalling and enhancing material efficiency of lightweight ultra high-performance concrete. *Cement Concrete Res* 158: 106842. <https://doi.org/10.1016/j.cemconres.2022.106842>
118. Zhang D, Tan KH (2022) Fire performance of ultra-high performance concrete: Effect of fine aggregate size and fibers. *Arch Civ Mech Eng* 22: 116. <https://doi.org/10.1007/s43452-022-00430-8>
119. Jiao Y, Zhang Y, Guo M, et al. (2020) Mechanical and fracture properties of ultra-high performance concrete (UHPC) containing waste glass sand as partial replacement material. *J Clean Prod* 277: 123501. <https://doi.org/10.1016/j.jclepro.2020.123501>
120. Alateah AH (2023) Engineering characteristics of ultra-high performance basalt fiber concrete incorporating geranium plant waste. *Case Stud Constr Mat* 19: e02618. <https://doi.org/10.1016/j.cscm.2023.e02618>
121. Lyu X, Elchalakani M, Ahmed T, et al. (2023) Residual strength of steel fibre reinforced rubberised UHPC under elevated temperatures. *J Build Eng* 76: 107173. <https://doi.org/10.1016/j.jobe.2023.107173>
122. Lyu X, Ahmed T, Elchalakani M, et al. (2023) Influence of crumbed rubber inclusion on spalling, microstructure, and mechanical behaviour of UHPC exposed to elevated temperatures. *Constr Build Mater* 403: 133174. <https://doi.org/10.1016/j.conbuildmat.2023.133174>
123. Banerji S, Kodur V, Solhmirzaei R (2020) Experimental behavior of ultra high performance fiber reinforced concrete beams under fire conditions. *Eng Struct* 208: 110316. <https://doi.org/10.1016/j.engstruct.2020.110316>
124. Hou X, Ren P, Rong Q, et al. (2019) Comparative fire behavior of reinforced RPC and NSC simply supported beams. *Eng Struct* 185: 122–140. <https://doi.org/10.1016/j.engstruct.2019.01.097>
125. Du H, Zhang M (2020) Experimental investigation of thermal pore pressure in reinforced C80 high performance concrete slabs at elevated temperatures. *Constr Build Mater* 260: 120451. <https://doi.org/10.1016/j.conbuildmat.2020.120451>
126. Zhang B, Lin X, Zhang YX, et al. (2023) Microscale failure analysis of the ultra-high-performance polypropylene fibre reinforced concrete panel subjected to high thermal loading induced by fire exposure. *Eng Struct* 292: 116518. <https://doi.org/10.1016/j.engstruct.2023.116518>
127. Han FY, Tang JH, Ji XP, et al. (2024) Evaluating the fire resistance potential of functionally graded ultra-high performance concrete. *J Build Eng* 97: 110987. <https://doi.org/10.1016/j.jobe.2024.110987>
128. Wang Y, Liu F, Xu L, et al. (2019) Effect of elevated temperatures and cooling methods on strength of concrete made with coarse and fine recycled concrete aggregates. *Constr Build Mater* 210: 540–547. <https://doi.org/10.1016/j.conbuildmat.2019.03.215>
129. Kara IB (2021) Effects of cooling regimes on limestone rock and concrete with limestone aggregates at elevated temperatures. *Int J Rock Mech Min* 138: 104618. <https://doi.org/10.1016/j.ijrmms.2021.104618>
130. Awal AA, Shehu I, Ismail M (2015) Effect of cooling regime on the residual performance of high-volume palm oil fuel ash concrete exposed to high temperatures. *Constr Build Mater* 98: 875–883. <https://doi.org/10.1016/j.conbuildmat.2015.09.001>



131. Durgun MY, Sevinç AH (2019) High temperature resistance of concretes with GGBFS, waste glass powder, and colemanite ore wastes after different cooling conditions. *Constr Build Mater* 196: 66–81. <https://doi.org/10.1016/j.conbuildmat.2018.11.087>
132. Fehérvári S (2022) Effect of cooling methods on the residual properties of concrete exposed to elevated temperature. *Results Eng* 16: 100797. <https://doi.org/10.1016/j.rineng.2022.100797>
133. Qin H, Yang J, Yan K, et al. (2021) Experimental research on the spalling behaviour of ultra-high performance concrete under fire conditions. *Constr Build Mater* 303: 124464. <https://doi.org/10.1016/j.conbuildmat.2021.124464>
134. Yang J, Yan K, Doh JH, et al. (2023) Experimental study on shear performance of ultra-high-performance concrete beams at elevated temperatures. *Eng Struct* 291: 116304. <https://doi.org/10.1016/j.engstruct.2023.116304>
135. Ren P, Hou X, Cui Z, et al. (2021) Fire resistance evaluation and minimum reinforcement ratio for hybrid fibre-reinforced RPC beams under fire exposure. *J Build Eng* 44: 103216. <https://doi.org/10.1016/j.jobbe.2021.103216>
136. Ma XM, Pan JL, Cai JM, et al. (2022) A review on cement-based materials used in steel structures as fireproof coating. *Constr Build Mater* 315: 125623. <https://doi.org/10.1016/j.conbuildmat.2021.125623>
137. Hou W, Zhang G, He SH (2022) Fire resistance tests on prestressed concrete box girder with intumescent fire-retardant coatings. *Fire Technol* 58: 107–131. <https://doi.org/10.1007/s10694-021-01145-7>
138. Mathews ME, Kiran T, Anand N, et al. (2022) Effect of protective coating on axial resistance and residual capacity of self-compacting concrete columns exposed to standard fire. *Eng Struct* 264: 114444. <https://doi.org/10.1016/j.engstruct.2022.114444>
139. Hou XM, Ren PF, Rong Q, et al. (2019) Effect of fire insulation on fire resistance of hybrid-fiber reinforced reactive powder concrete beams. *Compos Struct* 209: 219–232. <https://doi.org/10.1016/j.compstruct.2018.10.073>
140. Ren PF, Hou XM, Zheng WZ, et al. (2020) Quantifying fire insulation effects on the fire response of hybrid-fiber reinforced reactive powder concrete beams. *Fire Technol* 56: 1487–1525. <https://doi.org/10.1007/s10694-019-00937-2>
141. Kahanji C, Ali F, Nadjai A, et al. (2018) Effect of curing temperature on the behaviour of UHPFRC at elevated temperatures. *Constr Build Mater* 182: 670–681. <https://doi.org/10.1016/j.conbuildmat.2018.06.163>
142. Chen TF, Gao XJ, Ren M (2018) Effects of autoclave curing and fly ash on mechanical properties of ultra-high performance concrete. *Constr Build Mater* 158: 864–872. <https://doi.org/10.1016/j.conbuildmat.2017.10.074>
143. Yan K, Yang JC, Doh JH, et al. (2021) Factors governing the fire response of prestressed reactive powder concrete beams. *Struct Concr* 22: 607–622. <https://doi.org/10.1002/suco.201900359>
144. Rong Q, Hou XM, Ge C (2020) Quantifying curing and composition effects on compressive and tensile strength of 160–250 MPa RPC. *Constr Build Mater* 241: 117987. <https://doi.org/10.1016/j.conbuildmat.2019.117987>
145. Peng GF, Niu XJ, Shang YJ, et al. (2018) Combined curing as a novel approach to improve resistance of ultra-high performance concrete to explosive spalling under high temperature and its mechanical properties. *Cement Concrete Res* 109: 147–158. <https://doi.org/10.1016/j.cemconres.2018.04.011>

146. Liu JC, Du LP, Yao Y, et al. (2024) A close look at fire-induced explosive spalling of ultra-high performance concrete: From materials to structures. *Arch Civ Mech Eng* 24: 124. <https://doi.org/10.1007/s43452-024-00942-5>
147. Mohd Faizal MJ, Hamidah MS, Muhd Norhasri MS, et al. (2016) Effect of clay as a nanomaterial on corrosion potential of steel reinforcement embedded in ultra-high performance concrete, In: Yusoff M, Hamid N, Arshad M, et al. *InCIEC 2015*, Springer, Singapore. [https://doi.org/10.1007/978-981-10-0155-0\\_57](https://doi.org/10.1007/978-981-10-0155-0_57)
148. Zaid O, Hashmi SRZ, El Ouni MH, et al. (2023) Experimental and analytical study of ultra-high-performance fiber-reinforced concrete modified with egg shell powder and nano-silica. *J Mater Res Technol* 24: 7162–7188. <https://doi.org/10.1016/j.jmrt.2023.04.240>
149. Holan J, Novak J, Müller P, et al. (2020) Experimental investigation of the compressive strength of normal-strength air-entrained concrete at high temperatures. *Constr Build Mater* 248: 118662. <https://doi.org/10.1016/j.conbuildmat.2020.118662>



AIMS Press

© 2025 the Author(s), licensee AIMS Press. This is an open access article distributed under the terms of the Creative Commons Attribution License (<http://creativecommons.org/licenses/by/4.0>)